Stable Hydrogen and Oxygen Isotopes Reveal Aperiodic Non-River Evaporative Solute Enrichment in the Solute Cycling of Rivers in Arid Watersheds

By

KESEGO PEARL LETSHELE

Submitted in partial satisfaction of the requirements for the degree of

MASTER OF SCIENCE

in

Earth and Planetary Science

in the

OFFICE OF GRADUATE STUDIES

of the

UNIVERSITY OF CALIFORNIA

DAVIS

Approved:

Eliot A. Atekwana, Chair

Isabel P. Montañez

Tessa M. Hill

Committee in Charge

2022

Table of Contents

Acknowledgements

I thank my advisor, Dr. Eliot Atekwana, and it was a great honor and pleasure to work under his guidance. I also thank my committee for their support and constructive feedback during my journey, not forgetting my family and friends who supported me when the road got tough. I also appreciate Sisterhood in Science for their assistance throughout my research. This dissertation is dedicated to the loving memory of my mother and grandfather.

This thesis is reproduced from the original publication: Letshele, K.P., Atekwana, E.A., Molwalefhe, L., Ramatlapeng, G.J. and Masamba, W.R., 2022. Stable hydrogen and oxygen isotopes reveal aperiodic non-river evaporative solute enrichment in the solute cycling of rivers in arid watersheds. *Science of The Total Environment*, p.159113.

Highlights

- The δD, $\delta^{18}O$ and total dissolved ions (TDI) were investigated along the Okavango River in arid Botswana.
- The $\delta^{18}O$ vs. δD of river samples plot along the Okavango Delta Evaporation Line due to evaporation.
- Downriver d-excess was depleted by -0.04‰ km^{-1} (R^2=0.94) and correlates to -0.29 mean TDI (R^2=0.97).
- A mean TDI-d-excess model supports evaporation and reveals aperiodic solute input into the river.
- The aperiodic solute input driven by annual pulse flooding is spatially and temporally variable.

Abstract

We investigated the spatial and temporal variations of the stable isotope composition of hydrogen (δD) and oxygen ($\delta^{18}O$) and the total dissolved ions (TDI) concentrations in the Okavango River flowing through the Okavango Delta (Delta) in the middle Kalahari Desert. We aimed to elucidate the role of evaporation in controlling river solute enrichment from water samples collected at a one- to two-month frequency from nine stations along a ~460 km river transect for one year. We found that the δD and $\delta^{18}O$ composition and the TDI concentrations increased downriver. Seasonal increases in the δD and $\delta^{18}O$ values and in the TDI concentrations during the hot, rainy season were subdued and decreased during the cool, dry season from pulse flooding. The δD and $\delta^{18}O$ composition of the river samples plot along the Okavango Delta Evaporation Line are consistent with evaporation. The effect of evaporation during river transit was related to the mean δD (δD = 0.07*River distance (km) – 37.9; $R^2 = 0.98$) and mean d-excess (d-excess = -0.04*River distance (km) + 9.9; $R^2 = 0.94$). The effect of evaporation on the river solute behavior was characterized by the mean d-excess and TDI concentrations (d-excess = -0.29*TDI (mg/L) + 15.0; $R^2 = 0.97$). Samples from this study and those compiled from published studies plot at greater than one sigma standard deviation above and below the mean TDI concentration vs. mean d-excess regression model line. We use the marked deviations from the mean TDI concentration vs. the mean d-excess regression model to suggest that additional solutes from river-floodplain-wetland-island interaction driven by pulse flooding are delivered into the river. While our findings support an evaporation-dominated solute enrichment during river transit at the seasonal scale, we conclude that intermittent hydrology (e.g., pulse flooding) plays an important role in the sub-seasonal spatiotemporal behavior of solutes in rivers in arid watersheds, which must be considered in solute cycling models.

Keywords: d-excess; Hydrologic perturbations; Total dissolved ions; Endorheic River basin; Okavango Delta; Botswana

1. Introduction

Rivers in arid environments serve as essential sources of water supply for domestic, agricultural, and industrial use and support aquatic ecosystems (Greve and Seneviratne, 2015; D'Odorico et al., 2018; Thorslund et al., 2021). However, rivers in arid watersheds are typically characterized by high evaporation rates (McMahon and Nathan, 2021; Simpson and Herczeg, 1991). Significant evaporation of river water affects water quality by causing salinization, which can have adverse effects on the freshwater supplies, the river recharge of groundwater, and on the aquatic flora and fauna (e.g., Humphries et al., 2014; Mosimane et al., 2017). Despite the significance of evaporation in controlling solute cycling and potentially causing salinization of river water resources in arid regions, the extent to which evaporation modifies river solute behavior remains poorly understood. Understanding the extent to which evaporation alters river chemistry will form the basis for developing robust river solute cycling models and contribute valuable knowledge for effective water resource management in arid regions.

In humid watersheds where evaporation rates are typically low, groundwater (baseflow) is the dominant source of solutes in rivers, which can be augmented by solutes in overland flow during seasons with high precipitation and/or snow melt (Grasby et al., 1999). Therefore, groundwater dominantly influences river chemistry in humid regions (Godsey et al., 2009; Rose et al., 2018; Zhi et al., 2019). Conversely, rivers in arid watersheds lack baseflow support of discharge where the groundwater tables are deep. Thus, rivers in arid watersheds are supported by overland flow and will continuously lose water to groundwater recharge (influent) and to the atmosphere by evaporation. In influent rivers, episodic precipitation and floods control the timing, frequency, and magnitude of water and solutes delivered to the rivers (Bruesewitz et al., 2015), causing highly

variable discharge and solute concentrations over space and time. Therefore, solute cycling models developed for humid rivers (e.g., Aulenbach and Hooper, 2006; Peters et al., 2006; Aulenbach et al., 2016) are not suitable for describing solute behavior in rivers in arid environments, mainly due to differences in hydrologic support of river discharge, intermittency of hydrology, and climate (Oromeng et al., 2021). To develop a better understanding that will form the basis of solute cycling models, we will need to know if evaporation is the sole factor controlling solute enrichment of river water. If not, we will need to find out what other factors affect solutes and what their spatial and temporal effects are.

To understand the processes controlling the behavior of solutes in rivers in arid watersheds, we must assess the role of evaporation and non-evaporative processes in the spatial and temporal evapoconcentration of solutes. The stable isotopic composition of hydrogen (δD) and oxygen ($\delta^{18}O$) of water is a valuable tool for assessing river water evaporation (Huang and Pang, 2012; Chen and Tian, 2021; Vystavna et al., 2021) because evaporation causes isotopic fractionation (Craig, 1961; Dansgaard, 1964). On a global basis, the relationship between the $\delta^{18}O$ and δD in precipitation defines the global meteoric water line (GMWL; $\delta D = 8\delta^{18}O + 10$) with a deuterium excess (d-excess) of 10 (Craig, 1961; Petit et al.,1991; Horita et al., 2018). The $\delta^{18}O$ vs. δD of river samples that plot with regression line slopes that are lower than that of the GMWL have been affected by evaporation. In these samples, the decrease in the d-excess below the global value of 10 is commensurate with the extent of evaporation (Ehhalt, 1966; Merlivat and Jouzel, 1979; Edirisinghe et al., 2017; Aron et al., 2021). In rivers in arid watersheds where evaporation is the sole control of the solute behavior, we anticipate that the extent of evapoconcentration of solutes in the river water will be reflected by the decrease of the d-excess below 10 (Masson-Delmotte et al., 2005; Froehlich et al., 2008). A bulk measure of the solute concentration in rivers is the total

dissolved ions (TDI) which is easily measured by electronic meters (Hem, 1985). Hence, TDI is a useful parameter in rivers, which together with the d-excess composition, can be used to assess the role of evaporation in river solute behavior. We hypothesize that if the enrichment of river solutes is only due to evaporation, then we will observe good collinear relationships between the $\delta^{18}O$, δD, and d-excess of river water with solute concentration increases. The lack of such relationships might highlight the role of non-river evaporation processes in solute enrichment and solute cycling.

We investigated the role of evaporation in the evapoconcentration of solutes in the Okavango River flowing through the Okavango Delta (Delta) in the middle Kalahari Desert in northwestern Botswana. The hydrology of the Delta is driven by an annual flood pulse from the upper watershed in Angola and by local rainfall. The Delta is subject to high rates of evapotranspiration (ET) which result in (1) the precipitation of salts on hundreds of thousands of vegetated islands (McCarthy and Ellery 1998; Gumbricht and McCarthy, 2003) and floodplains and (2) cause solute enrichment in isolated wetland pools scattered across the Delta wetlands (Dincer et al., 1979; McCarthy and Ellery, 1998). Previous studies of the chemistry of the Okavango River in the Delta suggest that the downriver progressive enrichment of solute concentrations (e.g., Ca, Si) are from ET (Dincer et al., 1979; Sawula and Martins, 1991; Masamba and Muzila, 2005; Mladenov et al., 2005; Mackay et al., 2011; Akoko et al., 2013; Gondwe et al., 2017; Mosimane et al., 2017; Oromeng et al., 2021). Yet the extent of river solute increases from evaporative and non-evaporative processes has not been investigated. Therefore, a major aim of this study was to assess the enrichment of river solutes because of evaporation using stable water isotopes. For other processes such as dissolution of salts and transpiration which can enrich solutes and not cause isotopic fractionation, their solute enrichment effect will be summed up by the total dissolved ions. In this study, we investigated if evaporation is the sole process causing downriver enrichment of solutes in the

Okavango River. We measured the δD and $\delta^{18}O$ composition and TDI concentrations of river water every one to two months for one year at nine spatially distributed stations along the Okavango River. We use the spatial and temporal variations in TDI concentrations and the δD and $\delta^{18}O$ composition to model and elucidate the role of evaporation in controlling river solute behavior. We found that evaporation during river transit dominates the solute enrichment on a seasonal basis. At a sub-seasonal scale, evaporated water enriched in solutes from isolated wetland pools and salts dissolved from river floodplains and islands in the Delta wetlands are delivered to the Okavango River by hydrologic perturbations driven by pulse flooding and seasonal rains.

2. Study area

2.1. Okavango Delta

The Okavango Delta (Delta) is in NW Botswana and is located towards the terminus of the endorheic Okavango River Basin (ORB) (Fig. 1). The Cuito River and the Cubango River which drain the Cuito and Cubango sub-basins in the upper watershed in Angola join to form the Okavango River which flows into the Delta at Mohembo in Botswana (McCarthy and Ellery, 1998; McCarthy et al., 2003; Wolski and Murray-Hudson, 2008). The Delta is divided into a Panhandle and a lower delta region (Stanistreet and McCarthy, 1993). The Okavango River flows for ~460 km from Mohembo at the inlet to the Delta, through the Panhandle and the lower delta region to the outlet of the Delta in Maun (McCarthy et al., 1997). The Panhandle is a ~6000 km^2 narrow valley with a topographic gradient of 1:5600 through which the Okavango River meanders extensively (McCarthy et al., 1997). At the end of the Panhandle, the Okavango River branches into several distributaries forming the lower delta. The lower delta is a topographically low gradient (1:3400) alluvial fan that covers an area of ~120,000 km^2 formed in the Quaternary half-

graben of Okavango Rift Zone (Hutchins, 1976; McCarthy et al.,1997; Modisi et al., 2000; McCarthy, 2006; Bufford et al., 2012).

2.2. Geology

The Cuito and Cubango sub-basins are found on the Precambrian Congo craton made up of crystalline metamorphic gneisses, quartzites and migmatites (Bereslawski, 1997; McCourt et al., 2013). The metamorphic crystalline rocks are overlain by the sedimentary rocks of the Karoo Supergroup and thick layers of unconsolidated sands, clays, lime rock and lateritic layers of the Kalahari Superior Formation (Bereslawski, 1997; Catuneanu et al., 2005; Jones, 2010). The geology of the lower ORB consists of crystalline Precambrian rocks of the Damara and Ghanzi-Chobe belt (Kampunzu et al., 2000; Modie, 2000). These crystalline rocks are overlain by thick Quaternary Kalahari sediments which consist of alluvial, swamp, lacustrine and fluvio-deltaic deposits. The superficial geology of the lower delta comprises alluvium and recent swamp sediments (McCarthy et al., 1993; Hutchins, 1976; Reeves, 1978; McCarthy et al., 1993; Flugel, 2014).

2.3. Climate

The upper watershed of the ORB in Angola experiences a temperate climate with annual rainfall reaching 1100 to 1300 mm. Daily temperatures range from 22 to 24 °C during the rainy season, whereas during the dry season, temperatures decrease to 15 to 17 °C (Steudel et al., 2013; Pombo et al., 2015). The Delta in the lower ORB is in an arid, steppe and hot climate (Peel et al., 2007). The annual rainfall in the Delta averages 450 mm/y, with 95% of the rain falling during the rainy season (Milzow et al., 2009). The hot rainy season is from November to March and mean daily temperatures during the rainy season range from 22 to 24°C. The cool, dry season is from

April to October and the mean daily temperatures range from 15 to 17°C. As a result of the high temperatures in the Delta, the potential evapotranspiration measured at 2172 mm exceeds the annual rainfall received in the region by a factor of ~4 (Wilson and Dincer, 1976).

2.4. Hydrology

The Cuito River and Cubango River in the upper watershed in Angola contribute about 45% and 55%, respectively, to the discharge of the Okavango River (Mendelsohn and el Obeid, 2004). The hydrology of the Delta is controlled by an annual flood pulse generated from rainfall in the Cuito and Cubango headwater catchments and by local rains (McCarthy and Ellery, 1998; McCarthy et al., 2003; Wolski et al., 2008; Mackay et al., 2011). The peak of the annual flood pulse arrives at the inlet to the Delta in March and takes about 4-6 months to travel from the proximal portion of the Delta in Mohembo to the distal portion of the Delta in Maun (McCarthy and Ellery, 1998). The timing of the arrival of the annual flood pulse in the Delta is out of phase with the local rainy season. The average annual discharge into the Delta is 1.01×10^{10} m^3 and ranges from 6.0×10^{9} to 1.64×10^{10} m^3 (McCarthy et al., 2000). The discharge estimates based on outflow measurements in the distal portion of the Delta in Maun have been used to suggest that about 95% or more of the river discharge into the Delta is lost to ET (Wilson and Dincer, 1976; McCarthy et al., 1991, Gumbricht and McCarthy, 2003; Wolski et al., 2006).

An important characteristic of the Delta is the presence of extensive vegetation which form the freshwater wetland complexes. The vegetation consists of grasses, reeds and giant sedges in the river channel and margins, as well as in the Delta wetlands (McCarthy et al., 1993; Ellery et al., 2003). The Delta wetlands have been divided into ecotones based on the geomorphological controls of the landscape and the hydroperiod (McCarthy and Ellery, 1998). The Panhandle is a permanently flooded ecotone. The Panhandle is characterized by numerous meander and meander

cutoffs. River channel widths can exceed 50 m, river depths average 1.5 m and the river flows at velocities ranging between 0.4 and 0.8 m/s (e.g., Wolski et al., 2006). The lower delta is made up of distributary channels that are characterized as permanent, seasonal, and occasional flooded ecotones. The permanent ecotones extend from the edge of the Panhandle through the upper portion of the lower delta where the wetland hydroperiod, river depths and river velocity are similar to those of the river in the Panhandle. In the permanent, seasonal and occasional flooded ecotones in the lower delta, the distributary channels average ~15 m wide, water depths average 1 m and the water flows at a velocity of 0.01 m/s (Wilson and Dincer, 1976; Wolski et al., 2006). In the seasonal and occasionally flooded ecotones, the flood water is trapped at several locations to form isolated pools such as Guma and Dungu lagoons that undergo ET (Hart, 1997). The water in these isolated wetland pools undergo ET until the next annual flooding replenishes the water lost to ET (McCarthy et al., 1991).

In both the Panhandle and the lower delta, several islands ranging from a few m^2 to 1000 km^2 occur in the Delta wetlands (McCarthy and Metcalfe, 1990; Gumbricht et al., 2004; Humphries et al., 2014). Vegetation on these islands transpire large amounts of water which induce inflow of river water towards and into the islands (McCarthy et al., 1993). An outcome of transpiration in addition to evaporation is the selective exclusion and precipitation of salts on the surfaces around the edges and centers of the islands (McCarthy and Ellery, 1998; Gumbricht and McCarthy, 2003).

3. Methodology

3.1. Sample collection and sample analyses

This study was conducted from January to October 2009. We collected 89 grab samples from nine select stations located along the Okavango River between the proximal and the distal portion

of the Delta (Fig. 1). The stations were located in Mohembo (18°16'33.1"S, 021°47'12.7"E), Shakawe (18°24'44.5"S, 021°53'09.4"E), Sepopa (18°44'44.07"S, 022°11'53.53"E), Guma (18°57'50.4"S, 022°22'39.93" E), Boro (19°50'39.6''S, 023°24'04.8''E), Maun (20° 00'18.14''S, 023°25'34.4''E), Tsanakona (20°02'26.9"S, 023°23'08.0"E), Toteng (20°21'32.0''S, 022°56'46.2''E), and Lake Ngami (20°26'07.6''S, 022°49'41.3''E). The samples were collected every one to two months (Table 1). The unfiltered river water was initially collected in 1 L leak proof HDPE bottles. The samples were stored in a refrigerator at the Okavango Research Institute, where aliquots were transferred into 25 mL scintillation vials with inverted cone closures and transported to the United States of America. The samples were filtered through 0.45 µM nylon filters using 10 mL plastic syringes and refrigerated until analyses.

The total dissolved ions (TDI) were measured using an Orion Star A212 benchtop conductivity/TDS meter calibrated according to the manufacturer's instructions. Measurement of the δD and $\delta^{18}O$ of the samples was carried out by the technique of Gehre et al. (2004) using a high-temperature conversion elemental analyzer (TC/EA) coupled to a Thermo Finnigan Delta Plus XL isotope ratio mass spectrometer. The isotope ratios are reported in the delta notation (δ) in per mil (‰):

$$\delta\ (‰) = \left(\left(R_{sample}/R_{standard}\right) - 1\right) x\ 1000$$

where R is the D/H or $^{18}O/^{16}O$ in the sample and standard. The δD and $\delta^{18}O$ are reported relative to Vienna Standard Mean Ocean Water (VSMOW). In-house standards routinely measured have precisions of better than 0.1‰ for $\delta^{18}O$ and 2.0‰ for δD.

3.2. Rainfall, temperature, and river discharge

Daily rainfall data recorded at Sexaxa (Okavango Research Institute) weather station (23°31'42.05" E, 19°54'7.89" S) during the period of this study was obtained from online archives of the Okavango Research Institute (http://www.okavangodata.ub.bw/ori/monitoring/rainfall/; accessed June 1, 2021). The hourly air temperature values for the Maun Airport station (23°25'12" S,19°58'48" E,) were downloaded from the World Weather Online website (https://www.worldweatheronline.com; accessed June 1, 2021). The daily river discharge into the Delta inlet in Mohembo (21°47'14.32" S, 18°16'32.64" E) and outlet in Maun (23°25'35.08" S, 20°0'17.03" E) was retrieved from online archives of Okavango Research Institute (http://www.okavangodata.ub.bw/ori; accessed June 1, 2021).

4. Results

The results of the daily rainfall, hourly air temperature, and daily discharge for the Okavango River are presented in Table S1. The spatial and temporal results of the δD and $\delta^{18}O$ and the TDI concentrations of the Okavango River across the Delta are presented in Table S2. The statistical summaries (mean, minimum, maximum, and standard deviation) of the hourly air temperature, monthly rainfall, instantaneous discharge, the δD and $\delta^{18}O$ and TDI concentrations are presented in Table 1.

4.1. Rainfall and air temperature

The total rainfall measured during the sampling period is 378 mm (Table 1). During our study, rain fell from January 2009 to March 2009. In January, the daily rainfall amount ranged from 7 to14 mm. It increased to a maximum of 51 mm in the mid-rainy season in January and February and decreased to the end of the rainy season in April (Fig. 2a). The dry season which spans April

to August, is shaded in the panels in Figure 2 (and Figures 3 and 4). During the dry season, there were two notable daily rain events of 15 mm in May and 30 mm in July.

The hourly air temperature during our study ranged from 4.0 to 39.0 °C and averaged 23.0 ±6.4 °C (Table 1). On a seasonal basis, the hourly temperatures increased from low values in June during the dry season to peak values in January during the rainy season, before decreasing to lower values during the dry season (Fig. 2b). The hourly temperatures in the rainy season were higher compared to those in the dry season.

4.2. River discharge

The instantaneous discharge of the Okavango River measured at Mohembo ranged from 132 to 969 m^3/s (Table 1). The discharge began to increase in late January 2009 in the middle of the rainy season and peaked in March 2009 at the end of the rainy season (Fig. 2c). The discharge decreased continuously during the dry season until October 2009 at the beginning of the rainy season, when the discharge reached its lowest level.

The instantaneous discharge of the Okavango River measured in Maun in the distal portion of the Delta ranged from 0.3 to 16 m^3/s and averaged 5.7 m^3/s (Table 1). River discharge was low from January to mid-May at ~0.3 m^3/s. In late May, the discharge rate increased during the dry season to peak discharge from the middle to the end of the dry season in July through August 2009 (Fig. 2d). The receding limb of the discharge hydrograph began to fall from August through October.

The peak discharge in Maun (Fig. 2d) is 16% of the peak discharge in Mohembo (Fig. 2c) and is out of phase relative to the timing of peak discharge in Mohembo by five months. Additionally,

the peak discharge in Maun (Fig. 2d) occurs during the dry season with little to no rainfall (Fig. 2a) in the Delta.

4.3. Spatial and temporal variations of δD and $\delta^{18}O$

The δD measured in river water across the Delta ranged from -51 to 19 ‰, and the $\delta^{18}O$ ranged from -7.6 to 7.2 ‰ (Table 1). The δD and $\delta^{18}O$ show complementary behavior, and we show the temporal variations in the δD for each river station in Figure 3. Across the Delta, the δD increased downriver, was more negative in the Panhandle (Fig. 3a-d) and became increasingly positive in the lower delta (Fig. 3e-h). Over time, the δD in the Panhandle stations show mostly temporal increases (Fig. 3a-d), whereas river samples from the lower delta showed marked decreases from May through August during the dry season (Fig. 3e-h). The δD measured for water in Lake Ngami ranged from -15 to 55 ‰, and the $\delta^{18}O$ ranged from -1.9 to 11.7 ‰. There are temporal decreases in the δD and $\delta^{18}O$ in Lake Ngami during the cool dry season and increases during the hot rainy season (Table S1).

4.4. Spatial and temporal variations of TDI concentrations

The TDI concentrations measured in river water across the Delta averaged 63.4 ±30.3 mg/L and ranged from 22.2 to 202.3 mg/L (Table 1). Over time, the TDI concentrations showed little temporal change in the Panhandle (Fig. 4a-d), while in the lower delta, the TDI concentrations progressively increase from February to May during the rainy season, decreased sharply in May and June in the dry season and then decreased slowly until the beginning of the rainy season in September (Fig. 4e-h). The TDI concentrations for Lake Ngami averaged 126.8 ±65.6 mg/L and ranged from 81.1 to 290.6 mg/L. The TDI concentrations in Lake Ngami progressively increase

until May during the dry season, decrease sharply in May and June and stayed nearly constant through the rainy season (Table S1).

5. Discussion

Our assessment of the Okavango River across the Okavango Delta documents downriver enrichment in the isotopic composition (δD; Fig. 3) and solute concentrations (TDI; Fig. 4). On a temporal basis, the isotopic composition of river water showed a slower rate of increase during the cool, dry season, and enrichment during the hot, rainy season (δD; Fig. 3). On the other hand, the TDI concentrations showed minor changes reflected mostly as dilution in the TDI concentrations in the Panhandle of the Delta (Fig. 4a-d). In contrast, the TDI concentrations in the lower delta showed temporal enrichment from the rainy season to the mid-dry season, followed by a decrease in TDI concentrations until the beginning of the next rainy season (Fig. 4e-h). The differences in the solute behavior in the Panhandle and the lower delta indicate that in this arid climate, the processes (e.g., evaporation) controlling the solute concentrations in the Panhandle vs. the lower delta may be different or that these processes, if the same, act to change river solutes concentrations to different extents. Thus, we need to establish that river water evaporation occurs and assess its spatial and temporal effects on river solute behavior.

5.1. Evidence of evaporation from the stable isotopic composition of Okavango River water

The spatial and temporal variations in the δD and $\delta^{18}O$ in rivers in arid watersheds can be driven by precipitation (ultimate source of river water) that varies by season and by isotopic enrichment from evaporation (Stewart, 1975; Simpson and Herczeg, 1991; Clark and Fritz, 1997; Huang and Pang, 2012; Chen and Tian, 2021; Jeelani et al., 2021). Conversely, the temporal variations in TDI concentrations can be driven by ET-induced chemical changes in the water

column, water-rock interactions, or hydrological transport of solutes from the watershed to the river (Ramatlapeng et al., 2021). In the Okavango River, the downriver enrichment in the δD and $\delta^{18}O$ have been attributed to evaporation (Akoko et al., 2013; Atekwana et al., 2016), and the downriver increases in the solute concentrations have been attributed to evapoconcentration (Sawula and Martins, 1991; McCarthy et al., 1993; Cronberg et al., 1996; Mackay et al., 2011; Akoko et al., 2013; Atekwana et al., 2016; Gondwe and Masamba, 2016; Mosimane et al., 2017; Oromeng et al., 2021). Previous studies that investigated the stable water isotopes and solute behavior of the Okavango River (Akoko et al., 2013; Atekwana et al., 2016; Ramatlapeng et al., 2021) did not assess how evapoconcentration changes both the solute concentrations and the stable water isotopes in space and time across the Okavango Delta. To evaluate the spatial and temporal effects of evaporation on both the δD and $\delta^{18}O$ and the TDI concentrations in the Okavango River, we must first establish evidence of evaporation of river water.

5.1.1. Spatial evaporation of Okavango River water

The Okavango Delta is subjected to high ET rates, and the potential ET exceeds precipitation by a factor of 4 (Wilson and Dincer, 1976). Evaporation causes isotopic fractionation, which enriches the δD and $\delta^{18}O$ in surface waters (Stewart, 1975; Simpson and Herczeg, 1991; Clark and Fritz, 1997; Huang and Pang, 2012; Chen and Tian, 2021). Evaporation will cause enrichment in the δD and $\delta^{18}O$ as the river water transits over ~460 km of river distance from the proximal portion of the Delta in Mohembo to the distal portion of the Delta in Maun. The δD and $\delta^{18}O$ of the Okavango River samples co-vary (Fig. 5). In Figure 5, we also show the global meteoric water line (GMWL; Craig, 1961) and the local meteoric water line (LMWL; Akondi et al., 2019; Ramatlapeng et al., 2021). The δD and $\delta^{18}O$ of the Okavango River samples plot below the GMWL and the LMWL. In fact, the δD and $\delta^{18}O$ of the samples plot along the trend of the Okavango Delta

Evaporation Line (ODEL), consistent with evaporation river water (Dincer et al., 1979; Atekwana et al., 2016; Akondi et al., 2019; Ramatlapeng et al., 2021). The Okavango River samples from the Panhandle plot at or near the intersection of the ODEL, the GMWL and the LMWL ($\delta^{18}O$ = -6.5 ‰ and δD = -40 ‰) and are less enriched compared to samples from the lower delta, which plot further from the Panhandle samples along the ODEL (Fig. 5). Lake Ngami is a terminal lake that receives Okavango River water (Meier et al., 2015) and it shows the most isotopically enriched samples (Fig. 5). The clustering of data at the intersection of the ODEL, GMWL, and LMWL (Fig. 5) is used by us to suggest that local rains have less impact on the isotopic composition of river water delivered into the Okavango Delta.

Although the relationship between the δD and $\delta^{18}O$ provides evidence for evaporation of Okavango River water, it does not provide insight into how evaporation causes the observed spatial variations in the isotopic composition of river water. We can assess the changes in the δD and $\delta^{18}O$ across the Okavango Delta from the relationship between the distance traveled by river water from the proximal portion of the Delta in Mohembo (0 km) downriver to each station from their corresponding δD or $\delta^{18}O$. We plot the river flow distance for each station vs. the mean δD (±standard deviation) for the corresponding station (Fig. 6a). Overall, there is isotopic enrichment in the mean δD of each station with distance in the downriver direction (least squares fit the regression line of distance vs. the mean δD is described by: *mean δD = 0.07 x river distance – 37.9*; R^2 = 0.98). We use the regression model results from the mean δD vs. river distance as evidence of the spatial component of evaporative enrichment along the Okavango River. We have plotted the δD vs. station distance along the Okavango River distance from previously published studies (Akoko et al., 2013; Meier et al., 2015; Atekwana et al., 2016; Ramatlapeng et al., 2021) in Figure 6a. We observed that some samples which: (1) plot beyond one sigma of the 95%

confidence interval of the mean of δD but mostly plot below the model line are samples from the Panhandle and (2) plot beyond one standard deviation of the model line of the mean δD and mostly above the model line are from the lower delta. The δD from previous studies (Akoko et al., 2013; Meier et al., 2015; Atekwana et al., 2016; Ramatlapeng et al., 2021) also show smaller variability in their values in the panhandle but much greater variability in their values in the lower delta (Fig. 6a). We attribute the differences in the distribution of the δD values from previous studies from our model behavior to natural isotopic variability of the river discharge into the Delta, seasonal rains, variability in the extent of evaporation and/or input of variably evaporated water into the river from the Delta wetlands.

To further characterize the effects of evaporation on the isotopic composition of the Okavango River, we use a model based on the d-excess parameter. A model based on the d-excess parameter provides additional insight into the predictive evaporative rate with distance. This is because the d-excess given as 10 (d-excess = $\delta D - 8 \times \delta^{18}O$) on a global basis is independent of the isotopic composition of precipitation (Dansgaard, 1964). We use the d-excess parameter because lower d-excess values indicate a greater extent of evaporation (e.g., Dansgaard, 1964; Huang and Pang, 2012). We plot the river flow distance to reach each station from the proximal station at Mohembo (0 Km) vs. the mean d-excess (±standard deviation) for each station (Fig. 6b). The d-excess decreases with distance, consistent with greater evaporation with time and distance traveled by the river. The least squares fit to the distance regression vs. the mean d-excess data is described by *mean d-excess = -0.04 x river distance + 9.9;* R^2 = 0.94. The regression model based on the distance vs. mean d-excess (Fig. 6b) is consistent with the downriver evaporation documented by the regression model based on the distance vs. mean δD (Fig. 6a) and supports our suggestion of a strong spatial evaporative enrichment along the Okavango River. The d-excess data from

previously published studies conducted along the Okavango River (Akoko et al., 2013; Meier et al., 2015; Atekwana et al., 2016; Ramatlapeng et al., 2021) are aligned with our mean d-excess model, and the samples that do not plot within one standard deviation of the model line plot mostly below the model line (Fig. 6b). The d-excess from previous studies also show limited variability in their values in the panhandle, but much greater variability in their values in the lower delta (Fig. 6b). We argue that the much greater variability in the d-excess in the lower delta compared to the Panhandle is clear evidence that the rate of evaporation which is highly dependent on the residence time of river in this hot climate may arise from multiple variably evaporated water reservoirs feeding the river over space (Simpson and Herczeg, 1991).

5.1.2. Temporal evaporation of Okavango River water

The climate of the Okavango Delta is characterized by two seasons: the rainy season, in part, captured in our study from January to March, and the dry season which spanned from April to September (Fig. 2a). During the rainy season, daily temperatures were hotter and averaged 26.0 ±5 ºC compared to the dry season, which was cooler, with average daily temperatures of 21.0 ±7 ºC (Fig. 2b). In principle, the hot wet season should cause greater evaporative enrichment in the δD and $\delta^{18}O$ of river water, compared to the cooler dry season. Additionally, given that estimates suggest that one third of the water input into the Okavango Delta is from rainfall (Milzow et al., 2009), we should expect the δD and $\delta^{18}O$ composition of the river water to be shifted by that of the local rain, which has a much broader range in the δD and $\delta^{18}O$ (Akondi et al., 2019). Yet we observe mostly enrichment of the δD and $\delta^{18}O$ of river water during the rainy season (Fig. 3), contrary to the expected lowering of the isotopic composition from local rains.

We observed a decreased rate of isotopic enrichment during the cool, dry season in the Panhandle (Fig. 3a-d) and a marked decrease in the isotopic composition during the cool, dry season in the lower delta (Fig. 3e-h). Although out of phase with the local rains, the extent to which the annual pulse flood into the Delta influences river δD and $\delta^{18}O$ will depend on the isotopic composition of the water in the flood pulse, the downriver enrichment of the isotopes by in-water column evaporation, and the mixing with water from evaporated isolated wetland pools brought into the river (Ramatlapeng et al., 2021).

5.1.3. Evaluating the effects of evaporation in the Okavango River on TDI concentrations

We assessed the evaporation of river water on TDI concentrations using the relationship between TDI concentrations and d-excess. The degree of d-excess decrease, which represents the extent of evaporation, should be related to increases in the concentrations of solutes in river water if the solute concentrations increases are solely driven by evaporation. We show a plot of the mean TDI (±standard deviation) concentrations vs. the mean d-excess (±standard deviation) for our stations in Figure 7. The mean TDI concentrations increase with decreasing mean d-excess is defined by the least squares regression: *mean d-excess = -0.29 x TDI concentration + 15;* R^2 = 0.97; solid line in Fig. 7). The regression model, based on the mean TDI concentrations, and the mean d-excess, is used to suggest that in general, evaporation is responsible for the enrichment of solutes spatially along the Okavango River in the Delta. In the relationship between the mean TDI concentrations vs. mean d-excess, the standard deviations of the TDI concentrations and d-excess data become greater in the downriver direction (Fig. 7).

In Figure 7, we show the TDI concentrations vs. d-excess calculated from the δD and $\delta^{18}O$ from published studies conducted in the Okavango River (Akoko et al., 2013; Meier et al., 2015; Atekwana et al., 2016; Ramatlapeng et al., 2021). Over the TDI concentration ranges observed in

these samples, there is an overall negative relationship with d-excess, where at a 95% confidence level, 83% of the samples fall outside one sigma of the model line developed from data from this study (solid line including shaded portion; Fig. 7). The relationship between the TDI concentrations and d-excess for Okavango River water collected and evaporated by Atekwana et al. (2016) are shown by a dotted line for river water collected from the proximal portion of the Delta in Mohembo and by a dashed line for river water collected at the distal portion of the Delta in Maun (Fig. 7). The relationship for the TDI concentrations vs. d-excess for the evaporated river water is negative and highly correlated for Mohembo (*d-excess = -1.12 x TDI concentration + 40.0*, $R^2 = 0.94$) and Maun (*d-excess = -0.46 x TDI concentration + 17.9*; $R^2 = 0.90$), consistent with solute concentrations enrichment by evaporation. We note that the slope and the intercept of the relationship between TDI concentrations vs. d-excess for evaporated river water from Mohembo is about twice that for evaporated river water from Maun (Fig. 7).

If the only factor causing TDI enrichment of the Okavango River was evaporation, then the relationship of the TDI concentrations vs. d-excess data from the Delta collected from the proximal portion at Mohembo and the distal portion at Maun should lie along the same regression model line (e.g., Huang and Pang, 2012), instead of showing two independent relationships (Fig. 7). The experimental evaporation of river water from Mohembo and Maun conducted by Atekwana et al. (2016) represents idealized evaporation. We argue then that the different regression lines of the evaporation models result not from the process of evaporation but from the differences in the TDI concentration values of the river water being evaporated. While the d-excess in river water is controlled by evaporation, starting values of TDI concentrations that are different will result in different slopes for the regression of TDI vs. d-excess. Thus, based on (1) the good but different linear relationships between TDI concentrations vs. d-excess for evaporated river water from

Mohembo and Maun (dotted line compared to the dashed line; Fig. 7) and (2) the fact that the regression model for evaporated river water from Mohembo and Maun exhibit a different evaporative behavior compared to the model regression from data collected in this study (solid line; Fig. 7), we suggest that this is evidence that more than one process controls the enrichment behavior of solutes in river water spatially and temporally across the Delta.

We note that the data from Akoko et al. (2013), Meier et al. (2015), Atekwana et al. (2016), and Ramatlapeng et al. (2021) do not all follow any of the three regression models: evaporated river water from Mohembo (dotted line) or Maun (dashed line), or the mean TDI vs. d-excess from this study (solid line) (Fig. 7). We observe that the data mostly plot below the regression model developed in this study, and that only 17% of the data are aligned with the model behavior developed by Atekwana et al. (2016) for evaporation of river water from Mohembo (Fig. 7). We confirm our earlier suggestion based on increasingly large variability (standard deviation) at higher TDI concentrations and the wide TDI concentration variations at decreasing d-excess, that other processes besides downriver evaporation in part control the TDI concentrations in the Okavango River. The study by Ramatlapeng et al. (2021) shows that during the annual pulse flooding, river water flowing through the Delta can "push" water from evaporated water stored in the floodplains and wetlands into the river (piston flow) during rising discharge from flooding and drain water from the wetlands into the river during flood recession. Studies have shown that solutes precipitate on the Okavango River floodplain and the Delta islands (Gumbricht and McCarthy, 2003; Gumbricht et al., 2004; Ramberg and Wolski, 2008; Mackay et al.,2011). Therefore, flooding of the floodplains and islands dissolve the salt precipitates, which, together with water from evaporated wetland pools, are drained into the river during flood recession (Oromeng et al., 2021; Ramatlapeng et al., 2021). This transport-dependent supply of solutes from the floodplains,

islands, and from variably evaporated water from the wetland pools to the river is variable in magnitude and timing. There is wide scatter of data on the plot of TDI concentrations vs. d-excess (Fig. 7) for the time series experiment from Ramatlapeng et al. (2021). In the Ramatlapeng et al. (2021) study, sampling was conducted at a single station in Maun at the outlet of the Okavango Delta and shows clear evidence that multiple factors including hydrology control the magnitude and timing of solute concentrations in the Okavango River.

5.2. Conceptual model of processes that change the isotopic composition of water and solute concentrations in the Okavango River

The results of this study can be summarized in a conceptual model which shows which processes change the isotopic composition and solute concentrations in river input within the Delta (Fig. 8). River water that enters the Delta from the upper watershed is from seasonal rains, the annual flood pulse, and perhaps groundwater (Mendelsohn and el Obeid, 2004). We suspect that groundwater plays a role in the influx of water into the Cuito River and Cubango River at baseflow between rainy seasons (Mendelsohn and el Obeid, 2004). The δD and $\delta^{18}O$ composition of river water delivered into the Delta is from a combination of seasonal rains, groundwater, and the flood pulse with a $\delta^{18}O$ range of -7.5 to 4.5‰ and δD range of -50 to -30‰ (Fig. 5). The average solute concentration entering the Delta at Mohembo is characterized by the mean of TDI concentration of 28 ± 4 mg/L and is within the range of 5.7 to 84 mg/L reported for river water entering the Delta in Mohembo (Oromeng et al., 2021). When the river water enters the Delta and flows towards the exit of the Delta, the isotopic composition is modified by evaporation, as evidenced by the spatial d-excess decrease predicted by the distance traveled by river water in the Delta (Fig. 6b). Additionally, the annual flood pulse and seasonal rains bring fresh water with an isotopic composition different from that of the Okavango River in the Delta. The water within the Delta

wetlands is water trapped from the previous year's pulse flood and seasonal rains, which undergo variable evaporation before the following year's pulse flooding event. During the annual flood pulse, the increasing water level from flooding will "push" evaporated isotopically enriched water with higher solute concentrations from the floodplains and wetlands at the flood front into the river (hydraulic piston flow; Ramatlapeng et al., 2021). Additionally, the pulse flood waters could mix with water in the floodplains and wetlands which is subsequently drained into the river during the flood recession. This residual water drained into the river during the flood recession will have an isotopic composition different from that of the flood pulse and the evaporated enriched water in the floodplains and wetlands.

Our conceptual model can be used to suggest that the isotopic composition of water exiting the Delta will range from that of evaporated river water flowing down the river distributary channels, water flushed from the floodplains and isolated wetland pools into the river channels at the flood front, to flood waters mixed with water in the floodplains and isolated wetland pools drained into the river channels during flood recession (Fig. 8). Because of the spatial heterogeneity of the isotopic composition of water in the floodplains, isolated pools, and that of the mixed water in the floodplain and wetland, it may be difficult to pinpoint where the various isotopic transformation of the water in the river at the different stations occur.

The increases in the solute concentrations in the river accompanied by enriched $\delta^{18}O$ and δD corresponding to low d-excess can be attributed to evaporation with increased river flow distance (Fig. 6b). In addition, enrichment of solutes in the river can occur from the influx of evaporated water from floodplains and wetland pools, which would be characterized by lower d-excess from evaporation. During the time between the annual flooding pulses, evaporation and transpiration induced salt precipitation on the floodplain, wetlands and islands (McCarthy et al., 1993;

Gumbricht and McCarthy, 2003; Zimmermann et al., 2006). In this instance, the dissolved precipitates will be associated with water whose isotopic composition is similar to the advancing flood in the absence of significant mixing with residual evaporated water. Finally, the freshwater from the annual floods and local rains can control the solute concentrations. The extent to which the new flood or rainwater dominates the solute behavior in the river will depend on the relative volumes of the residual water in the Delta wetlands that mix with the advancing flood or rain-induced overland flow. On a spatiotemporal basis, we do not know the volume of the residual water in the floodplains and wetlands relative to that of the fresh flood waters or rains. However, time series investigations of the solute behavior in the Okavango River indicate that the most dilute solute concentration in the river occur between August and September at the tail end of the hydrograph recession (Oromeng et al., 2021). We hypothesize that sampling during this time will capture the isotopic and solute composition of the annual flood.

6. Limitations of isotopic quantification of solute enrichment along the Okavango River

Our study provides insights into the spatial and temporal variability of the processes that control the solute behavior in a river in an arid watershed from the $\delta^{18}O$ and δD composition and the total dissolved ion concentrations. Stable isotopes are ideal for quantifying evaporation, as evaporation induces an isotopic fractionation effect that can be tied to evaporation using the d-excess parameter (e.g., Huang and Pang, 2012). We model the TDI concentrations and d-excess of river samples from our study and samples from other studies assuming only evaporation (Fig. 7). Additionally, our modeling assumes that the river water from the station at the entrance to the Delta to the station at the exit of the Delta is a "closed system". By "closed" we mean no additional water is introduced into the evaporating river system. This is not the case in the Okavango Delta,

as additional variable amounts of water stored in the floodplains and wetlands is introduced into the river to different spatial and temporal extents by flooding and flood recession (Ramatlapeng et al., 2021).

Moreover, variable evaporation and the mixing of flood waters and floodplain waters and waters in evaporated wetland pools can provide isotopic composition and solute concentration signals that will be significantly different from continuous river water evaporation effects. We have therefore used the mismatch in the relationship between the spatial evaporative isotopic enrichment of river water and the solute concentration enrichment to suggest that other processes besides in-river evaporation control river solute behavior. It is possible to model how evaporation changes the d-excess and TDI concentrations because the change in d-excess is independent of the starting value of hydrogen and oxygen isotope (see Huang and Pang, 2012). However, the modeling is sensitive to the starting solute concentration values, as shown by river water evaporation from Mohembo and Maun which show dissimilar slopes and intercepts (Fig. 7).

In our focus on evaporation as a process for solute enrichment in the Okavango River, we do not account for the contribution of transpiration and dissolution to the behavior of river solutes. The Okavango Delta wetlands are heavily vegetated, and rooted and emergent vegetation can remove water from the floodplains and wetlands which would increase solute concentrations. The effect of transpiration is documented on the numerous islands in the Delta wetland that have caused salts to precipitate along the edges and centers of islands (e.g., McCarthy et al., 1993). Transpiration causes water loss to the atmosphere. This process is isotopically non-fractionating (Wershaw et al., 1966; Thorburn et al., 1993; Williams and Ehleringer, 2000) and therefore is not accounted for in our TDI concentration vs. d-excess model (Fig. 7). The scatter of TDI concentration data relative to the d-excess data (Fig. 7) could be from the variability of the degree

of transpiration in the Delta that is not accounted for in our model, since transpiration only affects solutes and not the δD and $\delta^{18}O$ composition of water. Thus, in our model, the effect of evaporation has been coupled with transpiration (although not quantified) which we compare with total dissolved ions. In this case, we assumed the two processes are directly proportional. When the transpiration effect is removed, the solute chemistry will still produce the same spatial and temporal relationships. Studies conducted on the different ecotones in the Delta show similar solute chemistry, indicating that transpiration may be constant and, as indicated by Schlesinger and Jasechkob (2014), ET in deserts could be 51± 15% the value of precipitation. We assume that ET is likely constant in the Delta; however, our inability to account for transpiration effects in our solute behavior analysis in the Okavango River may be a major limitation.

An important aspect of the annual pulse flood is that it drives solute enrichment and dilutions across the Delta. Variably evaporated water in the floodplains and wetlands is pushed into the river to varying degrees across space based on the heterogeneous locations of the evaporated wetland pools (Fig. 8). We do not know the isotopic composition and the solute concentrations of the numerous sources of water and solutes driven into the river by hydrologic connection of the river to water and salt pools during pulse flooding. The annual pulse flood dissolves variable amounts of salts precipitated on the floodplains and hundreds of thousands of islands in the Delta wetlands. In this case, the isotopic composition of the flood water does not need to change, but the solute concentration will vary depending on the water-dissolved salt ratio. So, the annual flooding can cause variable isotopic depletion or enrichment of river water and enrichment and dilution of solutes over temporal and spatial scales in the Okavango River.

7. Conclusions

We investigated the spatial and temporal variations of the $\delta^{18}O$ and δD and their effect on the solute behavior in the Okavango River in the Okavango Delta in semi-arid Botswana. Our study showed enrichment in the solute concentrations, and in the isotopic composition of water as the river transits ~460 km from the inlet (Mohembo) to the outlet (Maun) of the Delta. The downriver enrichment of solute concentrations and $\delta^{18}O$ and δD is attributed to the long residence time of water which is continuously exposed to evaporation. During the annual pulse flooding, when solute stores in the adjacent watershed are connected to the river, dissolved salts from the floodplains and islands and "old", highly evaporated water in the floodplains and isolated wetland pools are flushed to the river to increase the solute concentrations and enrich the $\delta^{18}O$ and δD. We use our results to suggest that the evaporation effect is profound in the spatial and temporal solute behavior of the Okavango River over seasonal scales. In contrast, hydrology plays an important role in controlling the solute behavior and stable water isotopic variations at sub-seasonal scales.

Figures

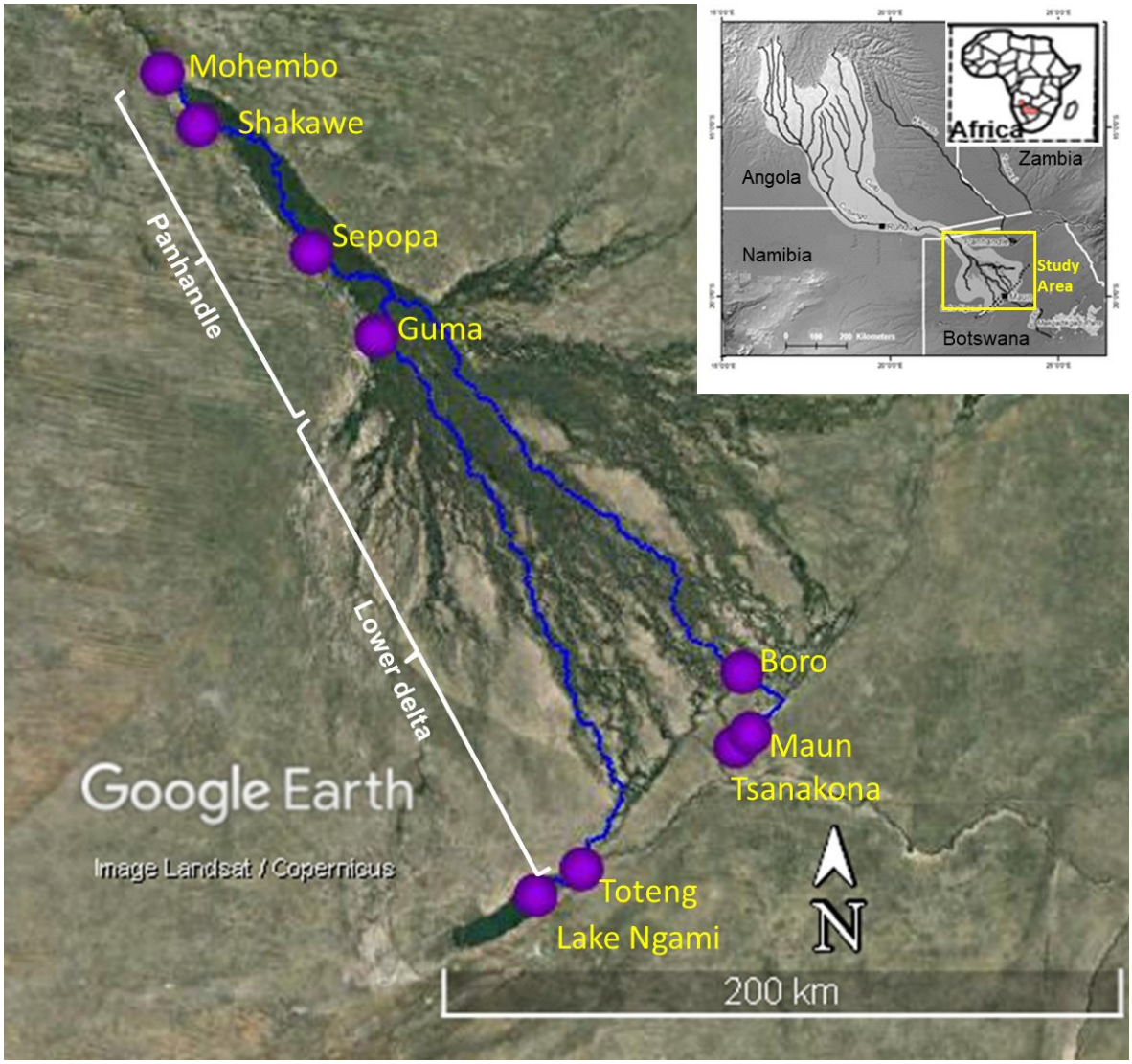

Figure 1: Google Earth™ image showing the Okavango Delta. Also shown are locations where water samples were collected for spatiotemporal investigation spanning the proximal portion of the Delta in Mohembo to the distal portion in the Delta at Maun and Ngami Lake. The inset shows the study area within the Okavango River Basin which is shown in the map of Africa in southern Africa (modified from Kgathi et al.,2006). The Okavango River Basin is modified from King and Chonguiça et al. (2016).

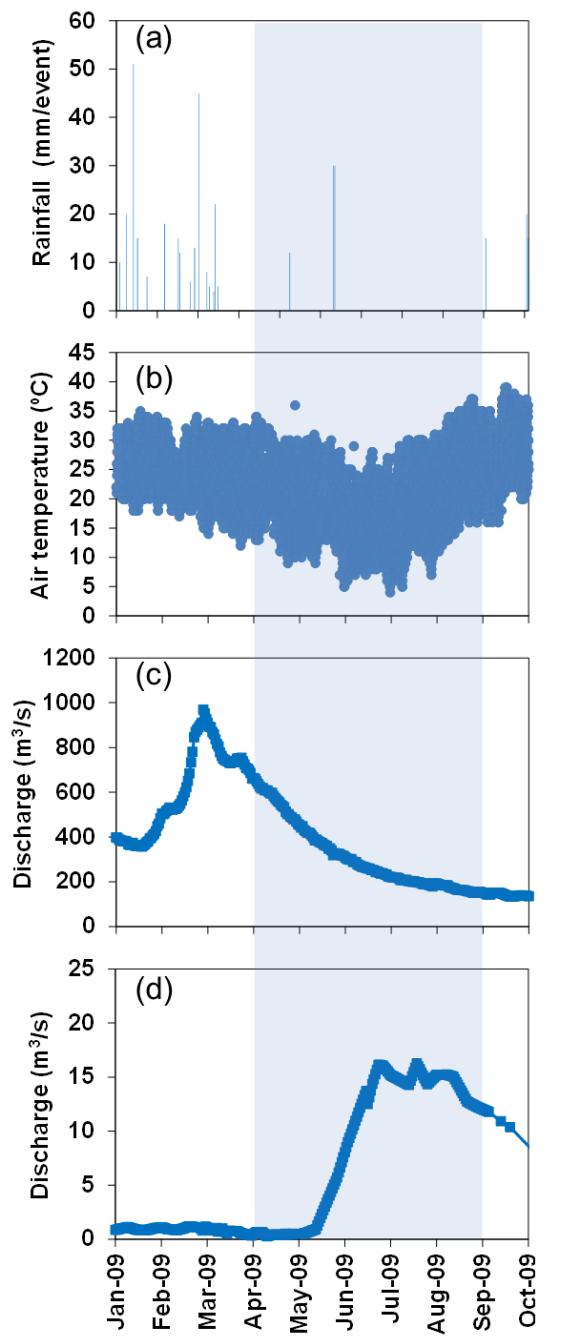

Figure 2: Temporal plot of daily rainfall (a), hourly air temperature (b) and daily discharge of the Okavango River at the proximal portion of the Delta in Mohembo (c) and at the distal portion of the Delta in Maun (d). The shaded region represents the dry season.

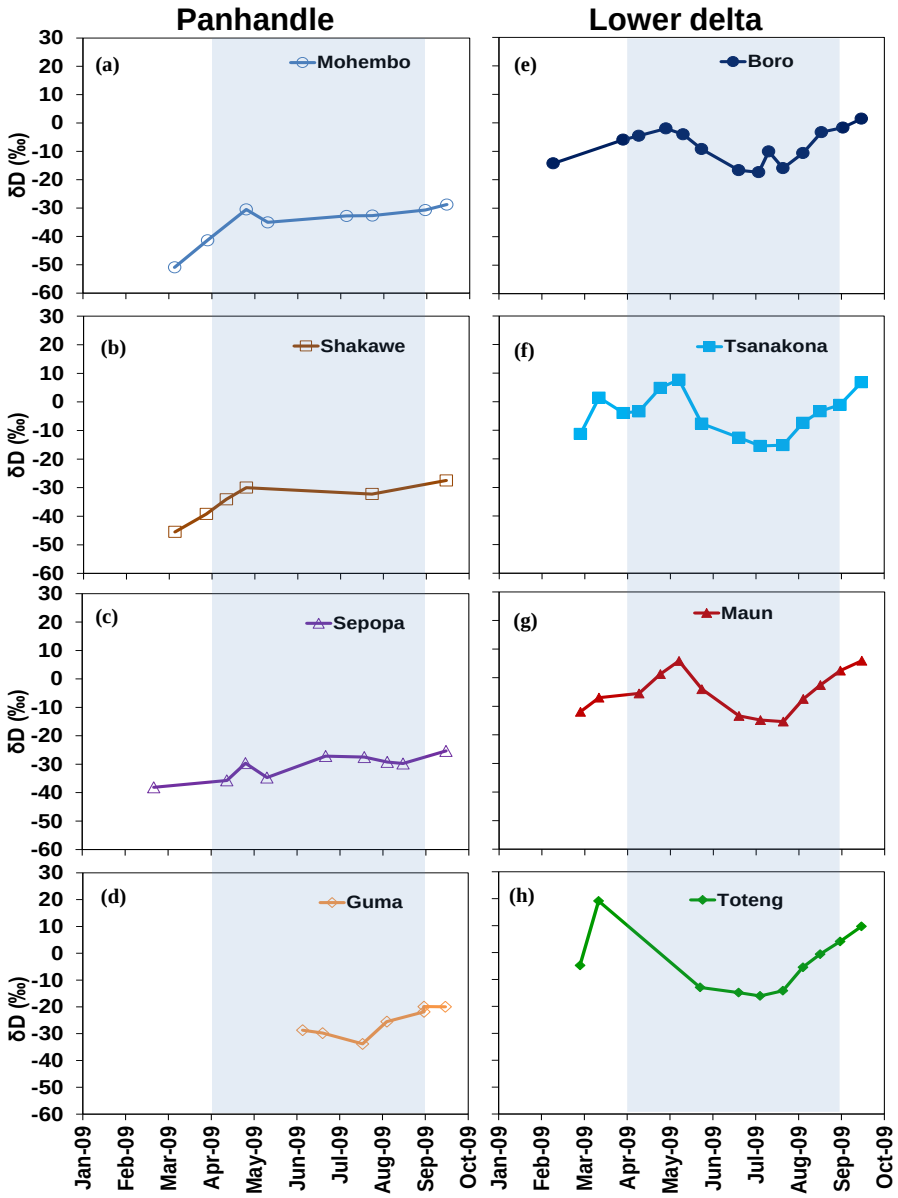

Figure 3: Temporal variations in the stable hydrogen isotopes (δD) at Mohembo (a), Shakawe (b), Sepopa (c) and Guma (d) in the Panhandle of the Okavango Delta and at Boro (e), Tsanakona (f) Maun (g), and Toteng (h) in the lower delta of the Okavango Delta. Sampling stations in the Panhandle are shown as open symbols and stations in the lower delta are shown as filled symbols. The shaded region on the panels depicts the dry season.

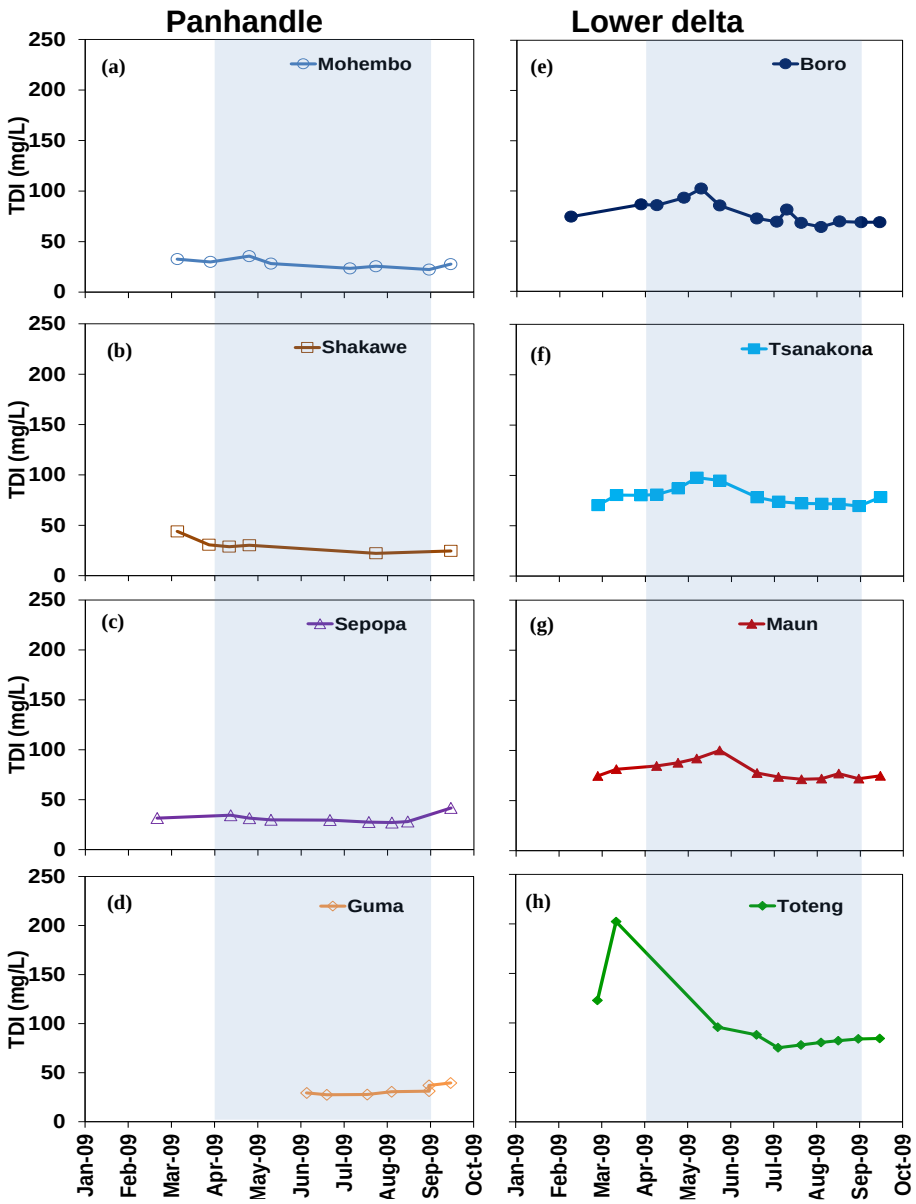

Figure 4: Temporal variations in the concentrations of total dissolved ions (TDI) at Mohembo (a), Shakawe (b), Sepopa (c) and Guma (d) in the Panhandle of the Okavango Delta and at Boro (e), Tsanakona (f) Maun (g), and Toteng (h) in the lower delta of the Okavango Delta. Sampling stations in the Panhandle are shown as open symbols and stations in the lower delta are shown as filled symbols. The shaded region on the panels depicts the dry season.

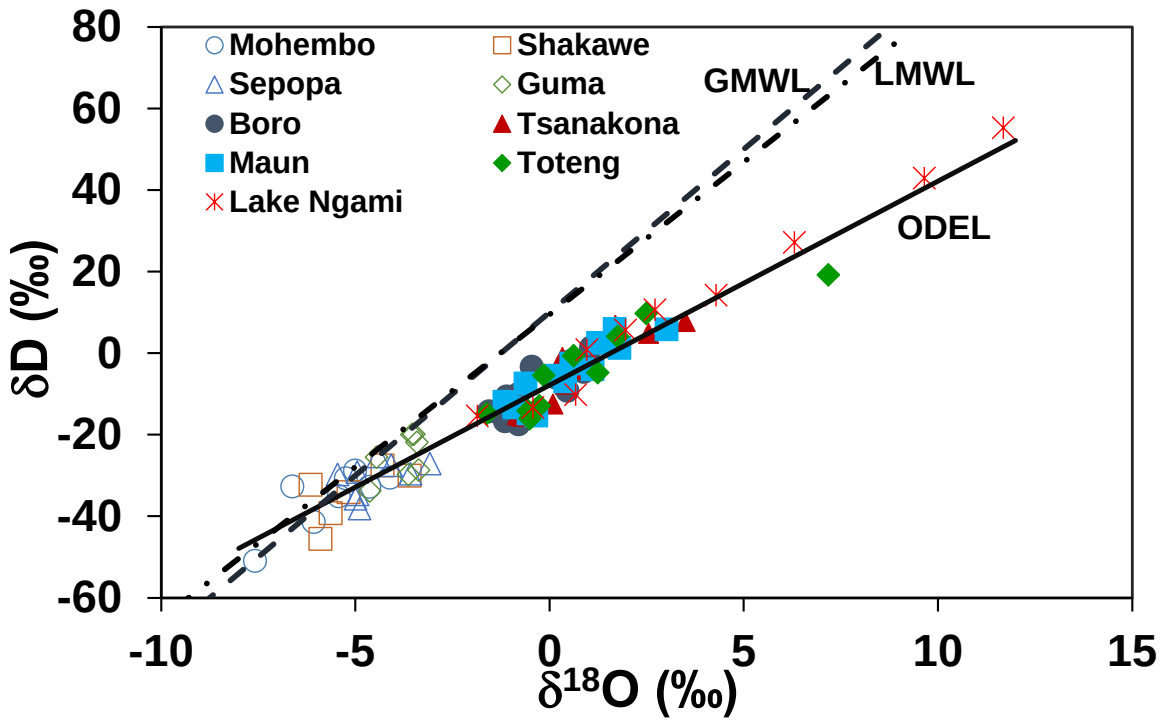

Figure 5**:** Cross plot of the stable oxygen isotopes ($\delta^{18}O$) vs. the stable hydrogen isotopes (δD) of samples from the Okavango River in the Okavango Delta. Stations in the Panhandle are shown as open symbols and stations in the lower delta are shown as filled symbols. Samples from Lake Ngami are shown as asterisk. Also shown is the Global Meteoric water line (GMWL; Craig Gordon, 1961), the Local Meteoric Water line (LMWL; Akondi et al., 2019) and the Okavango Delta Evaporation Line (ODEL; Atekwana et al., 2016).

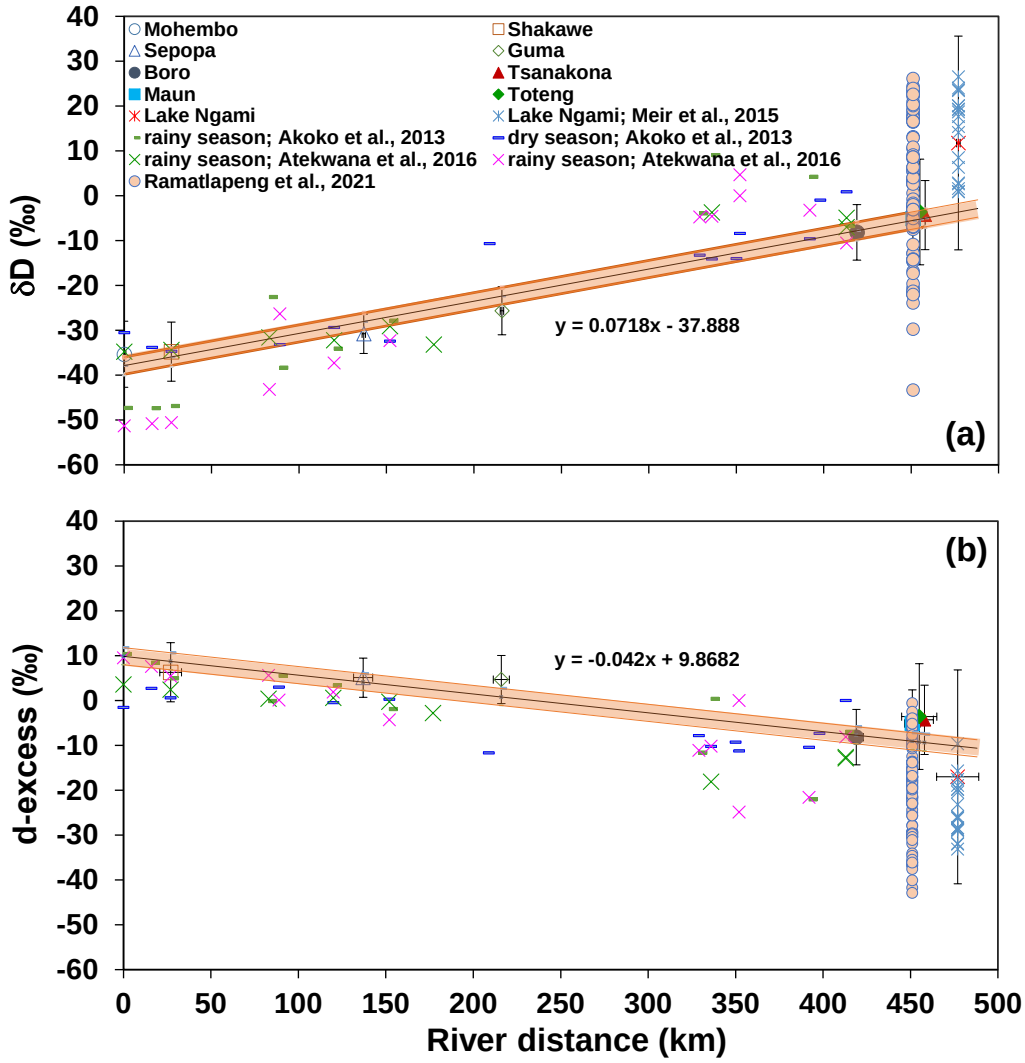

Figure 6**:** River distance traveled vs. δD (a) and river distance traveled vs. d-excess (b). Stations in the Panhandle are shown as open symbols and stations in the lower delta are shown as filled symbols. Samples from Lake Ngami are shown as asterisk. Data from published studies include Akoko et al. (2013), Meier et al. (2015), Atekwana et al. (2016) and Ramatlapeng et al. (2021). The solid line showing 1σ upper and low bound in brown shading is the regression model for the dD vs. distance (a) and d-excess vs. distance (b).

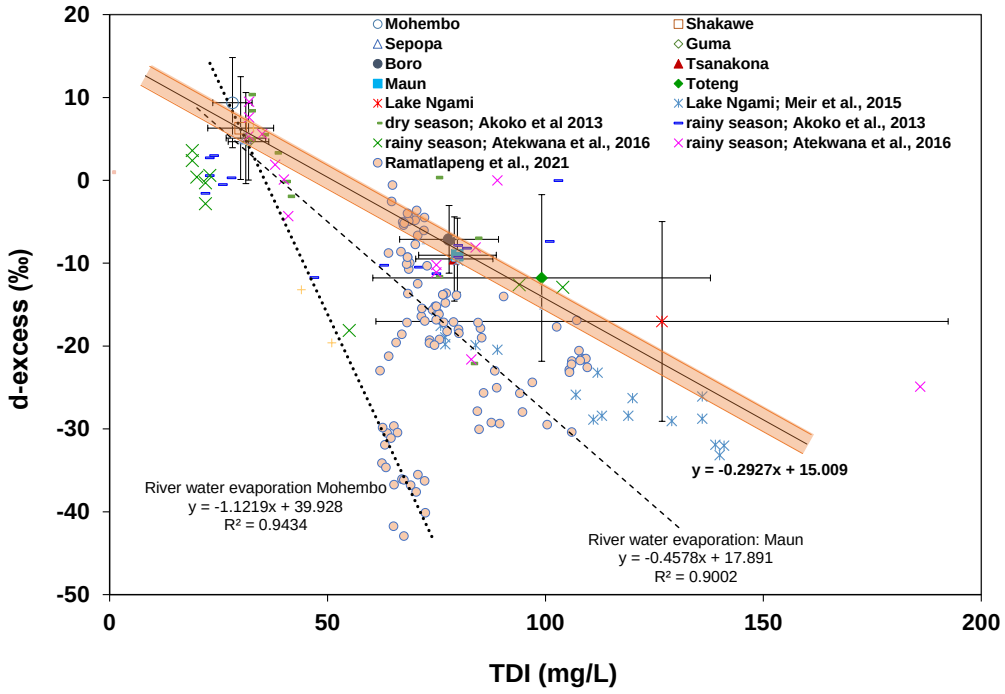

Figure 7**:** (a) Total dissolved ions (TDI) concentrations vs. d-excess. Stations in the Panhandle are shown as open symbols and stations in the lower delta are shown as filled symbols. Samples from Lake Ngami are shown as asterisks. Data from published studies include Akoko et al. (2013), Meier et al. (2015), Atekwana et al. (2016) and Ramatlapeng et al. (2021). The solid line showing 1σ upper and low bound in brown shading is the regression model from the mean TDI concentrations mean vs. d-excess and for the stations in this study. The dotted line and the dashed line are the regression model of TDI concentrations vs. d-excess for evaporated river water from Mohembo and Maun; respectively, from data presented in Atekwana et al. (2016).

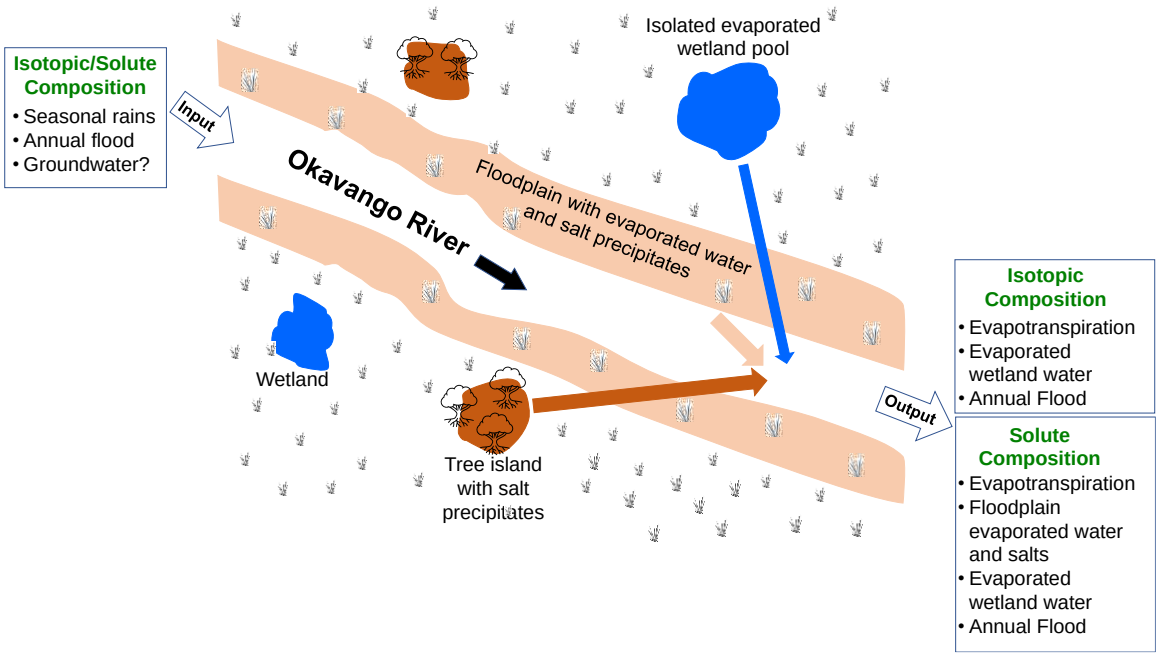

Figure 8**:** Conceptual model of how the stable oxygen and hydrogen isotopes and solutes in the Okavango River are changed during transit from the Delta inlet in Mohembo to the Delta exit at Maun.

Tables

Table 1**.** Statistical summary of air temperature, monthly rainfall, instantaneous discharge, stable hydrogen isotopes (δD) and stable oxygen isotopes ($\delta^{18}O$) and the total dissolved ions (TDI) concentrations from stations across the Okavango River.

Parameter	**Mean ± SD**	**Min**	**Max**
Air temperature (°C)	23 ± 6	4	39
Rainfall (mm)	1 ± 1	0	51
Discharge (Mohembo) (m^3/s)	385.77 ± 216.14	132.78	969.26
Discharge (Maun) (m^3/s)	5.68 ± 6.21	0.30	16.27
δD ($^0/_{00}$)	-15 ± 15	-51	19
$\delta^{18}O$ ($^0/_{00}$)	-1.4 ± 3.0	-7.6	7.2
TDI (mg/L)	63.4 ± 25.6	22.2	202.3

SD= Standard deviation, Min= Minimum, Max= Maximum

Table S1. Isotopic composition of hydrogen (δD), oxygen ($\delta^{18}O$) and concentrations of total dissolved ions across the Okavango River.

Location	Distance	Coordinates	Date sampled	$\delta^{18}O$ (‰)	δD (‰)	TDI (mg/L)
Mohembo	0	18°16'33.1"S,021°47'12.7"E	4/1/2009	-7.6	-51	32.6
Mohembo	0	18°16'33.1"S,021°47'12.7"E	4/24/2009	-6.1	-41	29.9
Mohembo	0	18°16'33.1"S,021°47'12.7"E	5/21/2009	-4.1	-30	35.6
Mohembo	0	18°16'33.1"S,021°47'12.7"E	6/5/2009	-5.4	-35	28.2
Mohembo	0	18°16'33.1"S,021°47'12.7"E	7/30/2009	-4.6	-33	23.5
Mohembo	0	18°16'33.1"S,021°47'12.7"E	8/17/2009	-6.6	-33	25.6
Mohembo	0	18°16'33.1"S,021°47'12.7"E	9/23/2009	-5.2	-31	22.3
Mohembo	0	18°16'33.1"S,021°47'12.7"E	10/8/2009	-5.0	-29	27.7
Shakawe	27	18°24'44.5"S,021°53'09.4"E	4/1/2009	-5.9	-45	43.9
Shakawe	27	18°24'44.5"S,021°53'09.4"E	4/23/2009	-5.6	-39	30.7
Shakawe	27	18°24'44.5"S,021°53'09.4"E	5/7/2009	-5.2	-34	28.8
Shakawe	27	18°24'44.5"S,021°53'09.4"E	5/21/2009	-3.6	-30	30.2
Shakawe	27	18°24'44.5"S,021°53'09.4"E	8/17/2009	-6.2	-32	22.2
Shakawe	27	18°24'44.5"S,021°53'09.4"E	10/8/2009	-4.3	-27	24.6

Sepopa	137	18°44'44.07"S,022°11'53.53"E	3/18/2009	-4.9	-38	31.6
Sepopa	137	18°44'44.07"S,022°11'53.53"E	5/8/2009	-5.0	-36	34.4
Sepopa	137	18°44'44.07"S,022°11'53.53"E	5/21/2009	-3.6	-30	31.5
Sepopa	137	18°44'44.07"S,022°11'53.53"E	6/5/2009	-4.9	-35	29.8
Sepopa	137	18°44'44.07"S,022°11'53.53"E	7/16/2009	-3.1	-27	29.6
Sepopa	137	18°44'44.07"S,022°11'53.53"E	8/12/2009	-4.1	-27	27.6
Sepopa	137	18°44'44.07"S,022°11'53.53"E	8/28/2009	-4.9	-29	27.1
Sepopa	137	18°44'44.07"S,022°11'53.53"E	9/8/2009	-5.5	-30	28.1
Sepopa	137	18°44'44.07"S,022°11'53.53"E	10/8/2009	-4.4	-25	41.7
Guma	216	18°57'50.4"S,022°22'39.93"E	6/30/2009	-3.4	-29	29.4
Guma	216	18°57'50.4"S,022°22'39.93"E	7/14/2009	-3.6	-30	27.4
Guma	216	18°57'50.4"S,022°22'39.93"E	8/11/2009	-4.6	-34	27.8
Guma	216	18°57'50.4"S,022°22'39.93"E	8/28/2009	-4.5	-25	30.6
Guma	216	18°57'50.4"S,022°22'39.93"E	9/23/2009	-3.4	-22	31.2
Guma	216	18°57'50.4"S,022°22'39.93"E	9/23/2009	-3.5	-20	37.1
Guma	216	18°57'50.4"S,022°22'39.93"E	10/8/2009	-3.5	-20	39.5
Boro	419	19°50'39.6"S,023°24'04.8"E	3/6/2009	-1.6	-14	74.4
Boro	419	19°50'39.6"S,023°24'04.8"E	4/24/2009	0.2	-6	86.6

Boro	419	19°50'39.6"S,023°24'04.8"E	5/5/2009	0.9	-5	85.8
Boro	419	19°50'39.6"S,023°24'04.8"E	5/24/2009	1.0	-2	93.1
Boro	419	19°50'39.6"S,023°24'04.8"E	6/5/2009	0.8	-4	102.3
Boro	419	19°50'39.6"S,023°24'04.8"E	6/18/2009	0.5	-9	85.5
Boro	419	19°50'39.6"S,023°24'04.8"E	7/14/2009	-1.2	-17	72.6
Boro	419	19°50'39.6"S,023°24'04.8"E	7/28/2009	-0.8	-17	69.3
Boro	419	19°50'39.6"S,023°24'04.8"E	8/4/2009	-0.8	-10	81.4
Boro	419	19°50'39.6"S,023°24'04.8"E	8/14/2009	-0.8	-16	68.1
Boro	419	19°50'39.6"S,023°24'04.8"E	8/28/2009	-1.1	-11	64.1
Boro	419	19°50'39.6"S,023°24'04.8"E	9/10/2009	-0.5	-3	69.6
Boro	419	19°50'39.6"S,023°24'04.8"E	9/25/2009	0.6	-2	68.8
Boro	419	19°50'39.6"S,023°24'04.8"E	10/8/2009	1.1	1	68.9
Maun	451	20°00'18.14"S,023°25'34.4"E	3/25/2009	-1.2	-12	74.6
Maun	451	20°00'18.14"S,023°25'34.4"E	4/7/2009	0.4	-7	81.2
Maun	451	20°00'18.14"S,023°25'34.4"E	5/5/2009	0.1	-6	84.5
Maun	451	20°00'18.14"S,023°25'34.4"E	5/20/2009	1.8	1	87.7
Maun	451	20°00'18.14"S,023°25'34.4"E	6/2/2009	3.0	6	92.0
Maun	451	20°00'18.14"S,023°25'34.4"E	6/18/2009	1.1	-4	100.0

Maun	451	20°00'18.14"S,023°25'34.4"E	7/14/2009	-0.9	-13	77.5
Maun	451	20°00'18.14"S,023°25'34.4"E	7/29/2009	-0.5	-15	73.6
Maun	451	20°00'18.14"S,023°25'34.4"E	8/14/2009	-0.3	-15	71.2
Maun	451	20°00'18.14"S,023°25'34.4"E	8/28/2009	-0.6	-7	71.8
Maun	451	20°00'18.14"S,023°25'34.4"E	9/9/2009	0.6	-3	76.9
Maun	451	20°00'18.14"S,023°25'34.4"E	9/23/2009	1.3	2	71.9
Maun	451	20°00'18.14"S,023°25'34.4"E	10/8/2009	1.7	6	74.7
Tsanakona	458	20°02'26.9"S,023°23'08.0"E	3/25/2009	-1.0	-11	70.4
Tsanakona	458	20°02'26.9"S,023°23'08.0"E	4/7/2009	1.7	1	80.5
Tsanakona	458	20°02'26.9"S,023°23'08.0"E	4/24/2009	0.8	-4	80.2
Tsanakona	458	20°02'26.9"S,023°23'08.0"E	5/5/2009	0.9	-3	81.0
Tsanakona	458	20°02'26.9"S,023°23'08.0"E	5/20/2009	2.6	5	87.1
Tsanakona	458	20°02'26.9"S,023°23'08.0"E	6/2/2009	3.5	8	97.8
Tsanakona	458	20°02'26.9"S,023°23'08.0"E	6/18/2009	0.4	-8	94.8
Tsanakona	458	20°02'26.9"S,023°23'08.0"E	7/14/2009	0.1	-13	78.1
Tsanakona	458	20°02'26.9"S,023°23'08.0"E	7/29/2009	-0.7	-15	73.9
Tsanakona	458	20°02'26.9"S,023°23'08.0"E	8/14/2009	-0.8	-15	72.1
Tsanakona	458	20°02'26.9"S,023°23'08.0"E	8/28/2009	-0.7	-7	71.8

Tsanakona	458	20°02'26.9"S,023°23'08.0"E	9/9/2009	0.2	-3	71.7
Tsanakona	458	20°02'26.9"S,023°23'08.0"E	9/23/2009	0.3	-1	69.5
Tsanakona	458	20°02'26.9"S,023°23'08.0"E	10/8/2009	1.7	7	78.4
Toteng	455	20°21'32.0"S,022°56'46.2"E	3/25/2009	1.2	-5	122.7
Toteng	455	20°21'32.0"S,022°56'46.2"E	4/7/2009	7.2	19	202.3
Toteng	455	20°21'32.0"S,022°56'46.2"E	6/17/2009	-0.3	-13	95.7
Toteng	455	20°21'32.0"S,022°56'46.2"E	7/14/2009	-1.6	-15	87.9
Toteng	455	20°21'32.0"S,022°56'46.2"E	7/29/2009	-0.5	-16	74.8
Toteng	455	20°21'32.0"S,022°56'46.2"E	8/14/2009	-0.5	-14	77.7
Toteng	455	20°21'32.0"S,022°56'46.2"E	8/28/2009	-0.1	-5	80.2
Toteng	455	20°21'32.0"S,022°56'46.2"E	9/9/2009	0.6	-1	82.0
Toteng	455	20°21'32.0"S,022°56'46.2"E	9/23/2009	1.8	4	83.8
Toteng	455	20°21'32.0"S,022°56'46.2"E	10/8/2009	2.5	10	84.3
Lake Ngami	477	20°26'07.6"S,022°49'41.3"E	3/25/2009	4.3	14.2	118.6
Lake Ngami	477	20°26'07.6"S,022°49'41.3"E	4/7/2009	6.3	27.2	147.8
Lake Ngami	477	20°26'07.6"S,022°49'41.3"E	4/23/2009	9.7	42.9	172.3
Lake Ngami	477	20°26'07.6"S,022°49'41.3"E	5/20/2009	11.7	55.3	290.6
Lake Ngami	477	20°26'07.6"S,022°49'41.3"E	6/17/2009	0.7	-10.2	119.7

Lake Ngami	477	20°26'07.6"S,022°49'41.3"E	7/14/2009	-1.9	-15.4	83.8
Lake Ngami	477	20°26'07.6"S,022°49'41.3"E	8/14/2009	-0.4	-13.4	82.9
Lake Ngami	477	20°26'07.6"S,022°49'41.3"E	9/9/2009	1.0	0.8	89.6
Lake Ngami	477	20°26'07.6"S,022°49'41.3"E	9/23/2009	2.0	5.6	81.1
Lake Ngami	477	20°26'07.6"S,022°49'41.3"E	10/8/2009	2.7	10.7	81.4

Table S2. Distance, Coordinates, Isotopic composition of oxygen ($\delta^{18}O$) and hydrogen (δD), calculated d-excess and concentrations of total dissolved ions (TDI) from published studies conducted in the Okavango River.

Station	Distance	Coordinates	$\delta^{18}O$ ($^0/_{00}$)	δD ($^0/_{00}$)	d-excess*	TDI (mg/L)
Akoko et.al 2013						
Low water						
Mohembo	0	18°16'37.98"S,21°47'12.04"E	-7.21	-47.33	10.35	32
Shakawe	16	18°21'36.94"S,21°50'46.70"E	-6.97	-47.37	8.39	32
Drosky	27	18°24'50.82"S,21°53'05.19"E	-6.48	-46.9	4.94	32
Mogotlho	83	18°32'01.49"S,22°09'19.01"E	-2.81	-22.62	-0.14	40
Mogacha	89	18°36'25.30"S,22°12'04.77"E	-5.48	-38.33	5.51	35
Sepopa	120	18°44'45.46"S,22°11'54.09"E	-4.68	-34.12	3.32	38
Seronga	152	18°49'18.87"S,22°24'52.72"E	-3.24	-27.85	-1.93	41
Boro	329	19°53'58.91"S,23°29'14.52"E	0.96	-3.96	-11.64	75
Maun	336	19°56'31.18"S,23°29'46.05"E	1.09	9.06	0.34	75
Kunyere	350	20°21'33.26"S,22°56'46.27"E				89
Komana	392	20°11'49.37"S,23°13'51.00"E	3.29	4.22	-22.1	83

Mababe	413	19°10'43.66"S,23°59'27.61"E	0.03	-6.75	-6.99	84
high water						
Mohembo	0	18°16'37.98"S,21°47'12.04"E	-3.62	-30.52	-1.56	22
Shakawe	16	18°21'36.94"S,21°50'46.70"E	-4.57	-33.83	2.73	23
Drosky	27	18°24'50.82"S,21°53'05.19"E	-4.41	-34.69	0.59	23
Mogacha	89	18°36'25.30"S,22°12'04.77"E	-4.52	-33.17	2.99	24
Sepopa	120	18°44'45.46"S,22°11'54.09"E	-3.61	-29.38	-0.5	26
Seronga	152	18°49'18.87"S,22°24'52.72"E	-4.09	-32.41	0.31	28
Lagoon	209	19°14'32.61"S,22°15'16.69"E	0.13	-10.67	-11.71	47
Boro	329	19°53'58.91"S,23°29'14.52"E	-0.67	-13.21	-7.85	80
Maun	336	19°56'31.18"S,23°29'46.05"E	-0.48	-14.09	-10.25	63
Kunyere	350	20°21'33.26"S,22°56'46.27"E	-0.59	-14.01	-9.29	80
Toteng	352	20°21'54.37"S,22°57'21.05"E	0.36	-8.38	-11.26	75
Komana	392	20°11'49.37"S,23°13'51.00"E	0.11	-9.58	-10.46	71
Mogotlho	398	19°14'25.55"S,23°57'16.03"E	0.8	-0.96	-7.36	101
Mababe	413	19°10'43.66"S,23°59'27.61"E	0.11	0.86	-0.02	103
Boteti	511	20°12'45.05"S,24°07'39.04"E	0.57	-3.61	-8.17	82

Meier et.al 2015

Lake Ngami

0	477	20°30'07.28"S,22°44'46.76"E	1.32	0.88	-9.7	80
1.94	477	20°30'07.28"S,22°44'46.76"E	2.16	1.6	-15.7	75
2.91	477	20°30'07.28"S,22°44'46.76"E	2.32	0.99	-17.6	76
4.22	477	20°30'07.28"S,22°44'46.76"E	2.7	2.67	-18.9	77
5.34	477	20°30'07.28"S,22°44'46.76"E	2.83	2.86	-19.8	77
6.28	477	20°30'07.28"S,22°44'46.76"E	3.28	6.36	-19.9	84
7.08	477	20°30'07.28"S,22°44'46.76"E	3.62	8.53	-20.4	89
8.28	477	20°30'07.28"S,22°44'46.76"E	5	14.13	-25.9	107
9.14	477	20°30'07.28"S,22°44'46.76"E	4.83	15.43	-23.2	112
10.22	477	20°30'07.28"S,22°44'46.76"E	5.79	20.05	-26.3	120
11.23	477	20°30'07.28"S,22°44'46.76"E	5.97	19.34	-28.4	119
12.11	477	20°30'07.28"S,22°44'46.76"E	5.76	17.67	-28.4	113
13.06	477	20°30'07.28"S,22°44'46.76"E	5.95	18.73	-28.9	111
13.96	477	20°30'07.28"S,22°44'46.76"E	6.03	19.21	-29.0	129
14.88	477	20°30'07.28"S,22°44'46.76"E	5.77	20.07	-26.1	136
15.74	477	20°30'07.28"S,22°44'46.76"E	6.53	23.47	-28.8	136

16.49	477	20°30'07.28"S,22°44'46.76"E	6.96	23.66	-32.0	141
17.25	477	20°30'07.28"S,22°44'46.76"E	6.99	24.01	-31.9	139
18.14	477	20°30'07.28"S,22°44'46.76"E	7.46	26.53	-33.2	140
Atekwana et.al 2016						
Mohembo	0	18°16'37.98"S,21°47'12.04"E	-4.8	-34.8	3.6	19
Drotsky	27	18°24'50.82"S,21°53'05.19"E	-4.6	-34.4	2.4	19
Mogotlho-Sangoshe	83	18°36'25.24"S,22°12'04.13"E	-4	-31.6	0.4	20
Sepupa	120	18°44'45.46"S,21°11'54.09"E	-4.1	-32.2	0.6	23
Seronga	152	18°49'19.30"S,22°24'51.79"E	-3.6	-29.1	-0.3	22
Qurube	177	19°14'46.17"S,22°15'11.85"E	-3.8	-33.2	-2.8	22
Maun	336	19°56'31.18"S,23°29'46.05"E	1.8	-3.7	-18.1	55
Kwai River Mababi	413	19°10'45.00"S,23°59'25.54"E	0.7	-7	-12.6	94
Mababe marsh	413	19°10'12.29"S,23°59'43.64"E	1	-4.9	-12.9	104
Mohembo	0	18°16'37.98"S,21°47'12.04"E	-7.6	-51.3	9.5	32
Shakawe	16	18°21'36.49"S,21°50'46.99"E	-7.3	-50.8	7.6	32
Drotsky	27	18°24'50.82"S,21°53'05.19"E	-7	-50.6	5.4	32
Mogotlho-Sangoshe	83	18°36'25.24"S,22°12'04.13"E	-6.1	-43.2	5.6	35
Mogotcha	89	18°39'46.90"S,22°15'54.67"E	-3.3	-26.3	0.1	40

Sepupa	120	18°44'45.46"S,21°11'54.09"E	-4.9	-37.3	1.9	38
Seronga	152	18°49'19.30"S,22°24'51.79"E	-3.5	-32.3	-4.3	41
Boro	329	19°53'59.25"S,23°29'14.29"E	0.8	-4.7	-11.1	75
Maun	336	19°56'31.18"S,23°29'46.05"E	0.7	-4.6	-10.2	75
Komana	392	20°11'49.63"S,23°13'51.97"E	2.3	-3.2	-21.6	83
Nhabe River Toteng	352	20°21'54.02"S,22°57'23.10"E	3.7	4.7	-24.9	186
Kunyere River Toteng	352	20°21'33.62"S,22°56'45.94"E	0	0	0	89
Kwai River Mababe	413	19°10'45.00"S,23°59'25.54"E	-0.3	-10.5	-8.1	84

Ramatlapeng et.al 2021

Maun

11/21/2017	451	19°57′16.77’,23°28′48.99″E	18.89	5.8416	-27.843	84.4
11/28/2017	451	19°57′16.77’,23°28′48.99″E	17.64	5.8578	-29.222	87.6
12/6/2017	451	19°57′16.77’,23°28′48.99″E	-21.91	-2.2861	-3.6218	70.45
12/13/2017	451	19°57′16.77’,23°28′48.99″E	20.934	6.2847	-29.344	89.5
12/20/2017	451	19°57′16.77’,23°28′48.99″E	23.19	6.653	-30.034	84.8
12/31/2017	451	19°57′16.77’,23°28′48.99″E	10.476	4.436	-25.012	88.85
1/6/2018	451	19°57′16.77’,23°28′48.99″E	8.2881	3.9088	-22.982	88.39
1/9/2018	451	19°57′16.77’,23°28′48.99″E	8.5621	4.2812	-25.688	94.15

1/13/2018	451	19°57′16.77’,23°28′48.99″E	2.6804	3.3811	-24.368	97
1/18/2018	451	19°57′16.77’,23°28′48.99″E	13.177	5.3323	-29.481	100.4
1/21/2018	451	19°57′16.77’,23°28′48.99″E	5.3833	4.1661	-27.945	94.75
1/26/2018	451	19°57′16.77’,23°28′48.99″E	-6.1479	0.9825	-14.008	90.4
1/28/2018	451	19°57′16.77’,23°28′48.99″E	12.951	5.4146	-30.365	106.05
2/1/2018	451	19°57′16.77’,23°28′48.99″E	17.287	4.272	-16.889	107.2
2/7/2018	451	19°57′16.77’,23°28′48.99″E	18.273	4.4925	-17.667	102.6
2/10/2018	451	19°57′16.77’,23°28′48.99″E	-43.328	-5.346	-0.5602	64.9
2/14/2018	451	19°57′16.77’,23°28′48.99″E	5.633	3.9097	-25.644	85.821
2/14/2018	451	19°57′16.77’,23°28′48.99″E	-20.585	-1.9715	-4.8133	70.1
2/19/2018	451	19°57′16.77’,23°28′48.99″E	-21.39	-2.0478	-5.0081	67.25
2/24/2018	451	19°57′16.77’,23°28′48.99″E	-19.587	-1.6177	-6.6453	70.7
2/28/2018	451	19°57′16.77’,23°28′48.99″E	-22.061	-2.2274	-4.2414	68.6
3/2/2018	451	19°57′16.77’,23°28′48.99″E	-29.744	-3.4012	-2.5349	64.7
3/5/2018	451	19°57′16.77’,23°28′48.99″E	-21.781	-2.1085	-4.9126	68.65
3/9/2018	451	19°57′16.77’,23°28′48.99″E	-21.6	-2.1401	-4.4785	72.25
3/12/2018	451	19°57′16.77’,23°28′48.99″E	-21.318	-1.9909	-5.3909	67.45
3/16/2018	451	19°57′16.77’,23°28′48.99″E	-23.915	-2.2362	-6.0255	72.15

3/19/2018	451	19°57′16.77’,23°28′48.99″E	-22.039	-2.259	-3.9676	68.35
3/23/2018	451	19°57′16.77’,23°28′48.99″E	-16.862	-1.0116	-8.7694	64
3/30/2018	451	19°57′16.77’,23°28′48.99″E	-14.573	-0.6644	-9.2574	68.4
4/2/2018	451	19°57′16.77’,23°28′48.99″E	-14.654	-0.7579	-8.5907	66.85
4/6/2018	451	19°57′16.77’,23°28′48.99″E	-12.773	-0.0382	-12.467	70.7
4/10/2018	451	19°57′16.77’,23°28′48.99″E	-12.888	-0.2743	-10.693	68.65
4/14/2018	451	19°57′16.77’,23°28′48.99″E	-14.255	-0.5382	-9.9495	68.9
4/17/2018	451	19°57′16.77’,23°28′48.99″E	-17.271	-0.8958	-10.105	68.15
4/21/2018	451	19°57′16.77’,23°28′48.99″E	-7.4806	1.2094	-17.156	68.25
4/24/2018	451	19°57′16.77’,23°28′48.99″E	-14.078	-0.6026	-9.2575	68.35
4/28/2018	451	19°57′16.77’,23°28′48.99″E	-10.881	0.3475	-13.66	68.45
5/1/2018	451	19°57′16.77’,23°28′48.99″E	2.5628	3.0441	-21.79	106.1
5/5/2018	451	19°57′16.77’,23°28′48.99″E	2.8245	3.0365	-21.468	108.3
5/8/2018	451	19°57′16.77’,23°28′48.99″E	3.3445	2.9849	-20.535	107.7
5/12/2018	451	19°57′16.77’,23°28′48.99″E	3.7197	3.1586	-21.549	108.95
5/15/2018	451	19°57′16.77’,23°28′48.99″E	3.6308	3.1422	-21.507	109.3
5/19/2018	451	19°57′16.77’,23°28′48.99″E	0.5717	2.9293	-22.862	105.5
5/22/2018	451	19°57′16.77’,23°28′48.99″E	3.6812	3.2797	-22.556	109.6

5/26/2018	451	19°57′16.77’,23°28′48.99″E	4.0208	3.22	-21.739	108
5/31/2018	451	19°57′16.77’,23°28′48.99″E	2.5994	3.0981	-22.185	106
6/6/2018	451	19°57′16.77’,23°28′48.99″E	4.0887	3.4054	-23.154	105.55
6/12/2018	451	19°57′16.77’,23°28′48.99″E	-5.0392	1.7791	-19.272	73.45
6/16/2018	451	19°57′16.77’,23°28′48.99″E	-5.5092	1.2111	-15.198	74.7
6/19/2018	451	19°57′16.77’,23°28′48.99″E	-6.2673	1.2654	-16.391	71.55
6/23/2018	451	19°57′16.77’,23°28′48.99″E	-6.5055	1.142	-15.641	74.1
6/26/2018	451	19°57′16.77’,23°28′48.99″E	-6.3363	1.6605	-19.621	73.4
6/30/2018	451	19°57′16.77’,23°28′48.99″E	-6.9879	1.2457	-16.953	72.35
7/3/2018	451	19°57′16.77’,23°28′48.99″E	-5.929	1.5074	-17.988	80.05
7/7/2018	451	19°57′16.77’,23°28′48.99″E	-6.8564	0.8753	-13.858	79.6
7/10/2018	451	19°57′16.77’,23°28′48.99″E	-3.0591	2.0171	-19.196	75.7
7/14/2018	451	19°57′16.77’,23°28′48.99″E	-2.4528	1.9974	-18.432	80.15
7/17/2018	451	19°57′16.77’,23°28′48.99″E	-2.6527	2.0416	-18.986	85.4
7/21/2018	451	19°57′16.77’,23°28′48.99″E	-4.1298	1.7125	-17.83	85.1
7/24/2018	451	19°57′16.77’,23°28′48.99″E	-3.8524	1.6634	-17.16	84.55
7/28/2018	451	19°57′16.77’,23°28′48.99″E	-3.3687	1.855	-18.208	77.45
7/31/2018	451	19°57′16.77’,23°28′48.99″E	-3.5041	1.408	-14.768	77.05

8/4/2018	451	19°57′16.77’,23°28′48.99″E	-2.4463	1.6929	-15.989	75.4
8/7/2018	451	19°57′16.77’,23°28′48.99″E	-2.6527	1.688	-16.156	75.6
8/11/2018	451	19°57′16.77’,23°28′48.99″E	-1.9948	1.6487	-15.184	75
8/14/2018	451	19°57′16.77’,23°28′48.99″E	-3.1687	1.3048	-13.607	77.25
8/18/2018	451	19°57′16.77’,23°28′48.99″E	6.2869	3.1076	-18.574	67.05
8/21/2018	451	19°57′16.77’,23°28′48.99″E	10.841	4.0065	-21.212	64.05
8/25/2018	451	19°57′16.77’,23°28′48.99″E	-2.1754	1.015	-10.295	72.85
8/28/2018	451	19°57′16.77’,23°28′48.99″E	-3.1881	0.568	-7.7318	70.15
9/1/2018	451	19°57′16.77’,23°28′48.99″E	-14.232	-1.1342	-5.1586	67.6
9/4/2018	451	19°57′16.77’,23°28′48.99″E	-0.7835	2.0393	-17.098	78.9
9/8/2018	451	19°57′16.77’,23°28′48.99″E	-1.6583	1.5186	-13.807	76.55
9/11/2018	451	19°57′16.77’,23°28′48.99″E	6.3286	3.6597	-22.949	62.05
9/15/2018	451	19°57′16.77’,23°28′48.99″E	-5.0752	1.2951	-15.436	71.65
9/18/2018	451	19°57′16.77’,23°28′48.99″E	9.1011	4.8419	-29.634	65.25
9/22/2018	451	19°57′16.77’,23°28′48.99″E	-2.8947	2.1226	-19.876	74.55
9/25/2018	451	19°57′16.77’,23°28′48.99″E	-2.0375	1.8855	-17.121	76.65
9/29/2018	451	19°57′16.77’,23°28′48.99″E	-3.0816	1.3405	-13.806	76.45
10/2/2018	451	19°57′16.77’,23°28′48.99″E	-3.0687	1.719	-16.82	74.95

10/6/2018	451	19°57′16.77’,23°28′48.99″E	6.4159	3.2479	-19.567	65.75
10/9/2018	451	19°57′16.77’,23°28′48.99″E	8.642	4.8906	-30.483	63.7
10/13/2018	451	19°57′16.77’,23°28′48.99″E	8.6108	4.8056	-29.834	62.65
10/16/2018	451	19°57′16.77’,23°28′48.99″E	17.697	7.4282	-41.729	65.16
10/21/2018	451	19°57′16.77’,23°28′48.99″E	22.558	7.8331	-40.107	72.46
10/23/2018	451	19°57′16.77’,23°28′48.99″E	17.418	6.1659	-31.91	63.16
10/27/2018	451	19°57′16.77’,23°28′48.99″E	16.621	5.8811	-30.428	66.08
10/30/2018	451	19°57′16.77’,23°28′48.99″E	16.453	5.9444	-31.103	64.55
11/3/2018	451	19°57′16.77’,23°28′48.99″E	19.3	7.0017	-36.714	65.26
11/6/2018	451	19°57′16.77’,23°28′48.99″E	22.189	7.3066	-36.264	72.28
11/10/2018	451	19°57′16.77’,23°28′48.99″E	24.388	7.6446	-36.77	69.09
11/13/2018	451	19°57′16.77’,23°28′48.99″E	20.125	6.7809	-34.122	62.5
11/17/2018	451	19°57′16.77’,23°28′48.99″E	16.604	6.4054	-34.64	63.41
11/20/2018	451	19°57′16.77’,23°28′48.99″E	26.151	7.9669	-37.584	70.35
11/24/2018	451	19°57′16.77’,23°28′48.99″E	23.239	8.2691	-42.913	67.53
11/27/2018	451	19°57′16.77’,23°28′48.99″E	20.359	7.0513	-36.052	67.09
12/1/2018	451	19°57′16.77’,23°28′48.99″E	23.94	7.431	-35.509	70.76
12/4/2018	451	19°57′16.77’,23°28′48.99″E	22.606	7.3426	-36.135	67.54

5/1/2019	451	19°57′16.77’,23°28′48.99″E	31.123	13.091	-73.603	106
5/7/2019	451	19°57′16.77’,23°28′48.99″E	-1.6964	3.1612	-26.986	74.38
5/10/2019	451	19°57′16.77’,23°28′48.99″E	22.83	11.02	-65.327	94.81
5/13/2019	451	19°57′16.77’,23°28′48.99″E	-7.8984	1.479	-19.731	71.51
5/17/2019	451	19°57′16.77’,23°28′48.99″E	36.248	14.995	-83.712	104
5/19/2019	451	19°57′16.77’,23°28′48.99″E	23.441	10.69	-62.083	88.12
5/23/2019	451	19°57′16.77’,23°28′48.99″E	27.769	12.074	-68.823	160.9
5/27/2019	451	19°57′16.77’,23°28′48.99″E	-3.182	1.7768	-17.396	64.57
5/31/2019	451	19°57′16.77’,23°28′48.99″E	39.152	15.01	-80.931	107.4
6/3/2019	451	19°57′16.77’,23°28′48.99″E	-11.985	-1.003	-3.9608	63.2
6/7/2019	451	19°57′16.77’,23°28′48.99″E	5.4321	3.6403	-23.69	54.68
6/10/2019	451	19°57′16.77’,23°28′48.99″E	9.4175	4.6207	-27.548	57.74
6/14/2019	451	19°57′16.77’,23°28′48.99″E	16.706	5.8847	-30.371	61.54
6/17/2019	451	19°57′16.77’,23°28′48.99″E	17.1	6.646	-36.068	54.77
6/21/2019	451	19°57′16.77’,23°28′48.99″E	4.0684	3.9351	-27.413	136.9
6/24/2019	451	19°57′16.77’,23°28′48.99″E	9.1334	4.5628	-27.369	56.71
6/28/2019	451	19°57′16.77’,23°28′48.99″E	0.5379	3.9001	-30.663	56.34
7/2/2019	451	19°57′16.77’,23°28′48.99″E	9.0359	5.0482	-31.35	57.05

7/9/2019	451	19°57′16.77’,23°28′48.99″E	13.957	5.7896	-32.36	59.38
7/12/2019	451	19°57′16.77’,23°28′48.99″E	11.021	5.1683	-30.326	57.79
7/16/2019	451	19°57′16.77’,23°28′48.99″E	14.345	6.2843	-35.93	124.1
7/20/2019	451	19°57′16.77’,23°28′48.99″E	7.9382	4.7387	-29.971	56.79
7/23/2019	451	19°57′16.77’,23°28′48.99″E	13.635	6.0083	-34.432	60.42
7/26/2019	451	19°57′16.77’,23°28′48.99″E	6.7393	5.0039	-33.292	57.39
7/29/2019	451	19°57′16.77’,23°28′48.99″E	16.272	6.423	-35.111	59.32
8/2/2019	451	19°57′16.77’,23°28′48.99″E	10.351	5.6044	-34.485	58.06
8/6/2019	451	19°57′16.77’,23°28′48.99″E	22.613	8.5534	-45.815	172.9
8/9/2019	451	19°57′16.77’,23°28′48.99″E	15.501	7.2487	-42.489	131

Acknowledgments

We thank the government of Botswana (Ministry of Education) for providing us with research permits. We thank an anonymous reviewer and the Associate Editor constructive comments that helped improved this manuscript.

CrediT authorship contribution statement

Kesego P. Letshele: Writing- Original draft, Conceptualization, Methodology, Data Analysis. **Eliot A. Atekwana:** Writing- reviewing and editing, Supervision, Funding Acquisition, Conceptualization, Methodology. **Loago Molwalefhe**: Writing-reviewing and editing, Conceptualization, Methodology. **Goabaone J. Ramatlapeng**: Writing-reviewing and editing, Methodology. **Wellington R. L. Masamba**: Writing-reviewing and editing, Sample collection.

Declaration of competing interest

The authors declare that they have no known competing financial interests or personal relationships that could have appeared to influence the work reported in this paper.

Disclosure statement

No potential conflict of interest was reported by the authors

Funding

This work was supported by the US National Science Foundation under Grant OISE-0927841.

References

Akoko, E., Atekwana, E.A., Cruse, A.M., Molwalefhe, L. and Masamba, W.R., 2013. River-wetland interaction and carbon cycling in a semi-arid riverine system: the Okavango Delta, Botswana. Biogeochemistry, 114(1-3), pp.359-380.

Akondi, R.N., Atekwana, E.A. and Molwalefhe, L., 2019. Origin and chemical and isotopic evolution of dissolved inorganic carbon (DIC) in groundwater of the Okavango Delta, Botswana. Hydrological Sciences Journal, 64(1), pp.105-120.

Aron, P.G., Levin, N.E., Beverly, E.J., Huth, T.E., Passey, B.H., Pelletier, E.M., Poulsen, C.J., Winkelstern, I.Z. and Yarian, D.A., 2021. Triple oxygen isotopes in the water cycle. Chemical Geology, 565, p.120026.

Atekwana, E.A., Molwalefhe, L., Kgaodi, O. and Cruse, A.M., 2016. Effect of evapotranspiration on dissolved inorganic carbon and stable carbon isotopic evolution in rivers in semi-arid climates: The Okavango Delta in North West Botswana. Journal of Hydrology: Regional Studies, 7, pp.1-13.

Aulenbach, B.T. and Hooper, R.P., 2006. The composite method: An improved method for stream-water solute load estimation. Hydrological Processes: An International Journal, 20(14), pp.3029-3047.

Bereslawski, E., 1997. Geohydrology, Geology, and Soils of the Cubango River Basin (Angolan Sector). OKACOM Okavango River Basin Preparatory Assessment Study, Specialist's Report.

Bruesewitz, D.A., Gardner, W.S., Mooney, R.F. and Buskey, E.J., 2015. Seasonal water column NH4+ cycling along a semi-arid sub-tropical river–estuary continuum: responses to episodic events and drought conditions. Ecosystems, 18(5), pp.792-812.

Bufford, K.M., Atekwana, E.A., Abdelsalam, M.G., Shemang, E., Atekwana, E.A., Mickus, K., Moidaki, M., Modisi, M.P. and Molwalefhe, L., 2012. Geometry and faults tectonic activity of the Okavango Rift Zone, Botswana: Evidence from magnetotelluric and electrical resistivity tomography imaging. Journal of African Earth Sciences, 65, pp.61-71.

Catuneanu, O., Wopfner, H., Eriksson, P.G., Cairncross, B., Rubidge, B.S., Smith, R.M.H. and

Chen, Y. and Tian, L., 2021. Canal surface evaporation along the China's South-to-North Water Diversion quantified by water isotopes. Science of the Total Environment, 779, p.146388.

Clark, I.D., Fritz, P., 1997. Environmental isotopes in hydrogeology. CRC Press.

Craig, H., 1961. Isotopic variations in meteoric waters. Science 133 (3465), 1702–1703.

Cronberg, G., Gieske, A., Martins, E., Nengu, J.P., Stenström, I.M., 1996. Major ion chemistry, plankton, and bacterial assemblages of the Jao/Boro River, Okavango Delta, Botswana: the swamps and flood plains. Archiv für Hydrobiologie. Supplementband. Monographische Beiträge 107 (3), 335–407

Dansgaard, W., 1964. Stable isotopes in precipitation. Tellus 16 (4), 436–468.

Dincer, T., Hutton, L.G. and Kupee, B.B.J., 1979. Study, using stable isotopes, of flow distribution, surface-groundwater relations and evapotranspiration in the Okavango Swamp, Botswana. In Isotope hydrology 1978.

D'Odorico, P., Davis, K.F., Rosa, L., Carr, J.A., Chiarelli, D., Dell'Angelo, J., Gephart, J., MacDonald, G.K., Seekell, D.A., Suweis, S. and Rulli, M.C., 2018. The global food-energy-water nexus. Reviews of Geophysics, 56(3), pp.456-531.

Edirisinghe, E.A.N.V., Pitawala, H.M.T.G.A., Dharmagunawardhane, H.A. and Wijayawardane, R.L., 2017. Spatial and temporal variation in the stable isotope composition ($\delta^{18}O$ and $\delta^{2}H$) of rain across the tropical island of Sri Lanka. Isotopes in Environmental and Health Studies, 53(6), pp.628-645.

Ehhalt, D.H., 1966. Tritium and deuterium in atmospheric hydrogen. Tellus, 18(2-3), pp.249-255.

Ellery, W.N., McCarthy, T.S. and Smith, N.D., 2003. Vegetation, hydrology, and sedimentation patterns on the major distributary system of the Okavango Fan, Botswana. Wetlands, 23(2), pp.357-375.

Flugel, T.J., 2014. The evolution of the Congo-Kalahari Watershed: African mega-geomorphology.

Froehlich, K., Kralik, M., Papesch, W., Rank, D., Scheifinger, H. and Stichler, W., 2008. Deuterium excess in precipitation of Alpine regions–moisture recycling. Isotopes in Environmental and Health Studies, 44(1), pp.61-70.

Gehre, M., Geilmann, H., Richter, J., Werner, R.A., Brand, W.A., 2004. Continuous flow 2H/ 1H and 18O/16O analysis of water samples with dual inlet precision. Rapid Commun. Mass Spectrom. 18 (22), 2650–2660.

Godsey, S.E., Kirchner, J.W., Clow, D.W., 2009. Concentration–discharge relationships reflect chemostatic characteristics of US catchments. Hydrological Processes: An International Journal 23 (13), 1844–18

Gondwe, M.J. and Masamba, W.R.L., 2016. Variation of physico-chemical parameters along a river transect through the Okavango Delta, Botswana. African Journal of Aquatic Science, 41(2), pp.205-215.

Gondwe, M.J., Masamba, W.R. and Murray-Hudson, M., 2017. Water balance and variations of nutrients and major solutes along a river transect through the Okavango Delta, Botswana. Botswana Notes and Records, 49, pp.26-43.

Grasby, S.E., Hutcheon, I. and McFarland, L., 1999. Surface-water–groundwater interaction and the influence of ion exchange reactions on river chemistry. Geology, 27(3), pp.223-226.

Greve, P. and Seneviratne, S.I., 2015. Assessment of future changes in water availability and aridity. Geophysical Research Letters, 42(13), pp.5493-5499.

Gumbricht, T. and McCarthy, T.S., 2003. Spatial patterns of islands and salt crusts in the Okavango Delta, Botswana. South African Geographical Journal, 85(2), pp.164-169.

Gumbricht, T., McCarthy, J. and McCarthy, T.S., 2004. Channels, wetlands and islands in the Okavango Delta, Botswana, and their relation to hydrological and sedimentological processes. Earth Surface Processes and Landforms: The Journal of the British Geomorphological Research Group, 29(1), pp.15-29.

Hart, R.C., 1997. A limnological profile of the upper Okavango Delta at low water level. Southern African Journal of Aquatic Science, 23(2), pp.21-33.

Hem, J.D., 1985. Study and Interpretation of the Chemical Characteristics of Natural Water: USGS Water-Supply Paper 2254. US Geological Survey, Washington, DC

Horita, J., Driesner, T. and Cole, D.R., 2018. Hydrogen isotope fractionation in the system brucite-water±NaCl to elevated temperatures and pressures: Implications for the isotopic property of NaCl fluids under geologic conditions. Geochimica et Cosmochimica Acta, 235, pp.140-152.

Huang, T. and Pang, Z., 2012. The role of deuterium excess in determining the water salinization mechanism: a case study of the arid Tarim River Basin, NW China. Applied Geochemistry, 27(12), pp.2382-2388.

Humphries, M.S., McCarthy, T.S., Cooper, G.R.J., Stewart, R.A. and Stewart, R.D., 2014. The role of airborne dust in the growth of tree islands in the Okavango Delta, Botswana. Geomorphology, 206, pp.307-317.

Hutchins, D.G., 1976. A Summary of the Geology, Seismicity, Geomorphology, and Hydro-geology of the Okavango Delta. Vol. 7. Geological Survey Dept

Jeelani, G., Shah, R.A., Deshpande, R.D., Dimri, A.P., Mal, S. and Sharma, A., 2021. Isotopic analysis to quantify the role of the Indian monsoon on water resources of selected river basins in the Himalayas. Hydrological Processes, 35(11), p.e14406.

Jones, M.J., 2010. The groundwater hydrology of the Okavango basin. OKACOM Okavango River Basin Transboundary Diagnostical Analysis Technical Report, pp.1-83.

Kampunzu, A.B., Armstrong, R.A., Modisi, M.P. and Mapeo, R.B.M., 2000. Ion microprobe U・Pb ages on detrital zircon grains from the Ghanzi Group: implications for the identification of

a Kibaran-age crust in northwest Botswana. Journal of African Earth Sciences, 30(3), pp.579-587.

King, J. and Chonguiça, E., 2016. Integrated management of the Cubango-Okavango River basin. Ecohydrology & Hydrobiology, 16(4), pp.263-271.

Kgathi, D.L., Kniveton, D., Ringrose, S., Turton, A.R., Vanderpost, C.H., Lundqvist, J. and Seely, M., 2006. The Okavango; a river supporting its people, environment and economic development. Journal of Hydrology, 331(1-2), pp.3-17.

Mackay, A.W., Davidson, T., Wolski, P., Mazebedi, R., Masamba, W.R., Huntsman-Mapila, P. and Todd, M., 2011. Spatial and seasonal variability in surface water chemistry in the Okavango Delta, Botswana: a multivariate approach. Wetlands, 31(5), pp.815-829.

Mackay, A.W., Davidson, T., Wolski, P., Mazebedi, R., Masamba, W.R., Huntsman-Mapila, P. and Todd, M., 2011. Spatial and seasonal variability in surface water chemistry in the Okavango Delta, Botswana: a multivariate approach. Wetlands, 31(5), p.815.

Masamba, W.R.L., Muzila, A., 2005. Spatial and seasonal variation of major cation and selected trace metal ion concentrations in the Okavango-Maunachira-Khwai channels of the Okavango Delta. Botswana Notes Rec. 37 (1), 218–226.

Masson-Delmotte, V., Jouzel, J., Landais, A., Stievenard, M., Johnsen, S.J., White, J.W.C., Werner, M., Sveinbjornsdottir, A. and Fuhrer, K., 2005. GRIP deuterium excess reveals rapid and orbital-scale changes in Greenland moisture origin. Science, 309(5731), pp.118-121.

McCarthy, J.M., Gumbricht, T., McCarthy, T., Frost, P., Wessels, K. and Seidel, F., 2003. Flooding patterns of the Okavango wetland in Botswana between 1972 and 2000. Ambio: A journal of the human environment, 32(7), pp.453-457.

McCarthy, T.S. and Ellery, W.N., 1998. The Okavango Delta. Transactions of the Royal Society of South Africa, 53(2), pp.157-182.

McCarthy, T.S., Metcalfe, J., 1990. Chemical sedimentation in the semi-arid environment of the Okavango Delta, Botswana. Chem. Geol. 89 (1-2), 157–178.

McCarthy, T.S., 2006. Groundwater in the wetlands of the Okavango Delta, Botswana, and its contribution to the structure and function of the ecosystem. Journal of Hydrology, 320(3-4), pp.264-282.

McCarthy, T.S., Barry, M., Bloem, A., Ellery, W.N., Heister, H., Merry, C.L., Röther, H. and Sternberg, H., 1997. The gradient of the Okavango fan, Botswana, and its sedimentological and tectonic implications. Journal of African Earth Sciences, 24(1-2), pp.65-78.

McCarthy, T.S., Ellery, W.N. and Ellery, K., 1993. Vegetation-induced, subsurface precipitation of carbonate as an aggradational process in the permanent swamps of the Okavango (delta) fan, Botswana. Chemical Geology, 107(1-2), pp.111-131.

McCarthy, T.S., McIver, J.R. and Verhagen, B.T., 1991. Groundwater evolution, chemical sedimentation and carbonate brine formation on an island in the Okavango Delta swamp, Botswana. Applied Geochemistry, 6(6), pp.577-595.

McCarthy, TS, Cooper, GRJ, Tyson, PD &Ellery, W., 2000. Seasonal flooding in the Okavango Delta, Botswana-recent history and future prospects. South African Journal of Science, 96(1), pp.25-33.

McCourt, S., Armstrong, R.A., Jelsma, H. and Mapeo, R.B.M., 2013. New U–Pb SHRIMP ages from the Lubango region, SW Angola: insights into the Palaeoproterozoic evolution of the Angolan Shield, southern Congo Craton, Africa. Journal of the Geological Society, 170(2), pp.353-363.

McMahon, T.A. and Nathan, R.J., 2021. Baseflow and transmission loss: A review. Wiley Interdisciplinary Reviews: Water, 8(4), p.e1527.

Meier, S.D., Atekwana, E.A., Molwalefhe, L. and Atekwana, E.A., 2015. Processes that control water chemistry and stable isotopic composition during the refilling of Lake Ngami in semi-arid northwest Botswana. Journal of Hydrology, 527, pp.420-432.

Mendelsohn, J., el Obeid, S., 2004. Okavango River: The Flow of a Lifeline. Struik, Cape Town.

Merlivat, L. and Jouzel, J., 1979. Global climatic interpretation of the deuterium-oxygen 18 relationship for precipitation. Journal of Geophysical Research: Oceans, 84(C8), pp.5029-5033.

Milzow, C., Kgotlhang, L., Bauer-Gottwein, P., Meier, P. and Kinzelbach, W., 2009. Regional review: the hydrology of the Okavango Delta, Botswana-processes, data and modelling. Hydrogeology Journal, 17(6), pp.1297-1328.

Mladenov, N., McKnight, D.M., Wolski, P., Ramberg, L., 2005. Effects of annual flooding on dissolved organic carbon dynamics within a pristine wetland, the Okavango Delta, Botswana. Wetlands 25 (3), 622–638.

Modie, B.N., 2000. Geology and mineralisation in the Meso-to Neoproterozoic Ghanzi-Chobe Belt of northwest Botswana. J. Afr. Earth Sci. 30 (3), 467–474.

Modisi, M.P., Atekwana, E.A., Kampunzu, A.B. and Ngwisanyi, T.H., 2000. Rift kinematics during the incipient stages of continental extension: Evidence from the nascent Okavango rift basin, northwest Botswana. Geology, 28(10), pp.939-942.

Mosimane, K., Struyf, E., Gondwe, M.J., Frings, P., Van Pelt, D., Schaller, J., Wolski, P., Schoelynck, J., Conley, D.J. and Murray-Hudson, M., 2017. Variability in chemistry of surface and soil waters of an evapotranspiration-dominated flood-pulsed wetland: solute processing in the Okavango Delta, Botswana. Water SA, 43(1), pp.104-115.

Oromeng, K.V., Atekwana, E.A., Molwalefhe, L. and Ramatlapeng, G.J., 2021. Time-series variability of solute transport and processes in rivers in semi-arid endorheic basins: The Okavango Delta, Botswana. Science of The Total Environment, 759, p.143574.

Peel, M.C., Finlayson, B.L. and McMahon, T.A., 2007. Updated world map of the Köppen-Geiger climate classification. Hydrology and Earth System Sciences, 11(5), pp.1633-1644.

Peters, N.E., Shanley, J.B., Aulenbach, B.T., Webb, R.M., Campbell, D.H., Hunt, R., Larsen, M.C., Stallard, R.F., Troester, J. and Walker, J.F., 2006. Water and solute mass balance of five small, relatively undisturbed watersheds in the US. Science of the Total Environment, 358(1-3), pp.221-242.

Petit, J.R., White, J.W.C., Young, N.W., Jouzel, J. and Korotkevich, Y.S., 1991. Deuterium excess in recent Antarctic snow. Journal of Geophysical Research: Atmospheres, 96(D3), pp.5113-5122.

Pombo, S., de Oliveira, R.P. and Mendes, A., 2015. Validation of remote-sensing precipitation products for Angola. Meteorological Applications, 22(3), pp.395-409

Ramatlapeng, G.J., Atekwana, E.A., Molwalefhe, L. and Oromeng, K.V., 2021. Intermittent hydrologic perturbations control solute cycling and export in the Okavango Delta. Journal of Hydrology, 594, p.125968.

Ramberg, L. and Wolski, P., 2008. Growing islands and sinking solutes: processes maintaining the endorheic Okavango Delta as a freshwater system. Plant Ecology, 196(2), pp.215-231.

Reeves, C.V., 1978. A failed Gondwana spreading axis in southern Africa. Nature 273 (5659), 222–223.

Rose, L.A., Karwan, D.L. and Godsey, SEE, 2018. Concentration–discharge relationships describe solute and sediment mobilization, reaction, and transport at event and longer timescales. Hydrological processes, 32(18), pp.2829-2844.

Sawula, G. and Martins, E., 1991. Major ion chemistry of the lower Boro River, Okavango Delta, Botswana. Freshwater Biology, 26(3), pp.481-493.

Schlesinger, W.H. and Jasechko, S., 2014. Transpiration in the global water cycle. Agricultural and Forest Meteorology, 189, pp.115-117.

Simpson, H.J. and Herczeg, A.L., 1991. Stable isotopes as an indicator of evaporation in the River Murray, Australia. Water Resources Research, 27(8), pp.1925-1935.

Stanistreet, I.G. and McCarthy, T.S., 1993. The Okavango Fan and the classification of subaerial fan systems. Sedimentary Geology, 85(1-4), pp.115-133.

Steudel, T., Göhmann, H., Flügel, W.A. and Helmschrot, J., 2013. Assessment of hydrological dynamics in the upper Okavango River Basins. Biodiversity and Ecology, 5, pp.247-262.

Stewart, M.K., 1975. Stable isotope fractionation due to evaporation and isotopic exchange of falling waterdrops: Applications to atmospheric processes and evaporation of lakes. Journal of Geophysical Research, 80(9), pp.1133-1146.

Thomas, D., Thomas, D.S., Shaw, P.A., 1991. The Kalahari Environment. Cambridge University Press.

Thorburn, P.J., Walker, G.R. and Brunel, J.P., 1993. Extraction of water from Eucalyptus trees for analysis of deuterium and oxygen-18: laboratory and field techniques. Plant, Cell & Environment, 16(3), pp.269-277.

Thorslund, J., Bierkens, M.F., Oude Essink, G.H., Sutanudjaja, E.H. and van Vliet, M.T., 2021. Common irrigation drivers of freshwater salinization in river basins worldwide. Nature Communications, 12(1), pp.1-13.

Vystavna, Y., Harjung, A., Monteiro, L.R., Matiatos, I. and Wassenaar, L.I., 2021. Stable isotopes in global lakes integrate catchment and climatic controls on evaporation. Nature Communications, 12(1), pp.1-7.

Wershaw, R.L., Friedman, IRVING, Heller, S.J. and Frank, P.A., 1966. Hydrogen isotopic fractionation of water passing through trees. Advanced in Organic Geochemistry, pp.55-67.

Williams, D.G. and Ehleringer, J.R., 2000. Intra-and interspecific variation for summer precipitation use in pinyon–juniper woodlands. Ecological Monographs, 70(4), pp.517-537.

Wilson, B.H. and Dincer, T., 1976, August. An introduction to the hydrology and hydrography of the Okavango Delta. In Symposium on the Okavango Delta (pp. 33-48). Botswana Soc. Gaborone Botswana.

Wolski, P. and Murray-Hudson, M., 2008. Alternative futures' of the Okavango Delta simulated by a suite of global climate and hydro-ecological models. Water SA, 34(5), pp.605–610

Wolski, P., Savenije, H.H., Murray-Hudson, M. and Gumbricht, T., 2006. Modelling of the flooding in the Okavango Delta, Botswana, using a hybrid reservoir-GIS model. Journal of Hydrology, 331(1-2), pp.58-72.

Zhi, W., Li, L., Dong, W., Brown, W., Kaye, J., Steefel, C. and Williams, K.H., 2019. Distinct source water chemistry shapes contrasting concentration-discharge patterns. Water Resources Research, 55(5), pp.4233-4251.

Zimmermann, S., Bauer, P., Held, R., Kinzelbach, W. and Walther, J.H., 2006. Salt transport on islands in the Okavango Delta: numerical investigations. Advances in Water Resources, 29(1), pp.11-29.